Bates College
SCARAB

Standard Theses | Student Scholarship

5-2017

# Late-Season High-Sedimentation Events in a Sediment Trap Record from Linnévatnet, Svalbard, Norway

Noel L. Potter
*Bates College*, noel.l.d.potter@gmail.com

Follow this and additional works at: http://scarab.bates.edu/geology_theses

Recommended Citation
Potter, Noel L., "Late-Season High-Sedimentation Events in a Sediment Trap Record from Linnévatnet, Svalbard, Norway" (2017). *Standard Theses*. 31.
http://scarab.bates.edu/geology_theses/31

This Open Access is brought to you for free and open access by the Student Scholarship at SCARAB. It has been accepted for inclusion in Standard Theses by an authorized administrator of SCARAB. For more information, please contact batesscarab@bates.edu.

# Late-Season High-Sedimentation Events in a Sediment Trap Record from Linnévatnet, Svalbard, Norway

A Senior Thesis

Presented to the Faculty of the Department of Geology, Bates College, in partial fulfillment of the requirements for the Degree of Bachelor of Science

by

Noel L. D. Potter

Lewiston, Maine

April 7th, 2017

# Abstract

Linnévatnet is a proglacial lake in the high Arctic, on the western coast of Spitsbergen, Svalbard, Norway. Svalbard's climate is warm for its high latitude, with temperatures increasing in recent years and expected to continue rising. Given the longer and more intense melt season brought about by a warming climate, overall sedimentation may increase, and a large portion of that increase may be due to late summer and fall "shoulder season" storms falling as rain more often than as snow. This study utilizes the annual sediment trap record for the 2015-'16 accumulation year in order to document the effects of such late-season events on sedimentation in Linnévatnet, where sediment cores have yielded important high-resolution paleoclimate records.

Sediment traps have been deployed in Linnévatnet since 2003, along with weather stations, time-lapse cameras, and an intervalometer, which records the timing of sediment deposition. Sediment traps are positioned to capture sediment in important zones of the lake, with special focus given to a transect from the primary inlet to the main basin. Studies of modern sedimentation patterns in the lake allow for better understanding and interpretation of sedimentary records of past climate.

Meteorological and intervalometer data indicate that a rainstorm on September 11-12, 2015 yielded nearly 70% of the year's total sediment. This contradicts the classic model of annually varved lake sediments, in which a nival flood of spring snowmelt carries most of the year's sediment. Downcore profiles of grain size and XRF profiles of Ca, Zr, Fe, and K content distinguish sediment associated with the September rainstorm from that associated with the nival pulse. Sediment from the September rainstorm likely traveled in an irregular plume, not reaching all parts of the lake. Signatures of the nival pulse, however, were seen in all sediment traps, with some minor variations in composition representing variations in source lithology. With 70% of the year's sediment associated with the September rainstorm, the characteristics unique to the fall storm had a significant influence on Linnévatnet's sedimentation for the year. If shoulder season rainstorms are becoming more prevalent, it could drastically alter the sedimentation patterns in lakes like Linnévatnet.

# Acknowledgements

I have many people to thank for their part in my experience writing this thesis and the process leading up to it. I'm sure I will miss some of you. Forgive me.

Thank you to all of the people involved in my field experience with AG-220 at UNIS: Johnny, Linn Tove, and the rest of the Isfjord Radio crew for giving us a cozy, welcoming place to stay at the end of the Earth; Sebastian, Sara, Lis, Wes, Lena, Steve, and Al, for your guideance, knowledge, and a lot of miles hiked; to my classmates, for sharing the work and making it not seem like work at all, and to Heather, Jack, Arnau, Lucy, Eicke, Lucien, Alex, and everyone else I got to know in my time in Longyearbyen, for giving me a home away from home in a little town in the Arctic.

To the professors in the Bates Geo Department and all of my other geology teachers and mentors throughout the years, thank you for giving me the background to embark on such a great project, and for the support before and during the thesis process.

To my fellow Bates Geo Majors, thank you for the support and friendship this year and throughout our four years – being able to share our courses and this thesis experience with you has made me a better geologist and let me enjoy it along the way.

To Hanna, Emma, and Angie, thank you for putting up with all of the maps, smelly hiking boots, bad puns (geology-related or otherwise), uncalled-for geologic enthusiasm, and for being there for the late nights and stress-inducing deadlines.

To Mike, my advisor, thank you for taking me to the Arctic, for guiding me up from Sed through two research projects and on to grad school applications, for our conversations from Townes van Zandt to the Sox, Bruins, and Pats to the latest "misguided" politician's take on climate change, and for helping me through the thesis process this year, even on my worst days of procrastination. Oh, and last, but definitely not least, thanks for all the Kvikk Lunsj bars.

Finally, to my parents, thank you for taking me outdoors early and often, for putting a (usually) good head on my shoulders, for encouraging me to find and do what works for me and supporting me as I do, for sending me off to the Arctic, and for… everything else too. Much love.

# A note to the reader

Many geographic features mentioned in this study are referred to by their Norwegian names. Thus, Linnévatnet is Lake Linné, Linnédalen is the Linné Valley, Kapp Linné is Cape Linné, Linnébreen is the Linné Glacier, and Linnéelva is the Linné River.

# Contents

# Table of Figures

# Chapter 1

# Introduction

# Purpose and Significance

In a rapidly changing global climate, the Arctic is warming especially quickly, a trend present in all seasons and for all atmospheric circulation patterns (e.g. Cohen, et al., 2014; Serezze and Barry, 2011; Kaufman, et al., 2009). As increasing greenhouse gas concentrations drive increasing surface air temperatures globally, the Arctic Ocean loses sea ice, a loss which in turn drives further warming in the Arctic. Sea ice insulates against heat exchange between cold Arctic air masses and relatively warmer open ocean waters, and its high albedo reflects much of the solar radiation the Arctic receives in summer. Conversely, the increased thermal exchange between open ocean waters and the increased absorption of solar radiation by open ocean waters associated with decreasing sea ice both lead to increased atmospheric warming (Serreze and Francis, 2006; Isaksen, et al., 2016). On Svalbard specifically, temperature anomalies have been uniformly positive since 2001 for all atmospheric circulation patterns and seasons, but anomalies are especially high in the winter months, when the effects of sea ice or its absence are most acutely felt (Isaksen, et al., 2016). The warmer temperatures and increased evaporation allowed by the reduced sea ice cover are producing increased precipitation and decreased snowfall fractions, amounting to significant increases in rainfall, especially during the late summer, fall, and early winter (Bintanja and Andry, 2017). Understanding the changes to the Arctic climate system is an important part of understanding the changing global climate and may help predict future climatic behavior. Arctic climate research is an essential component of efforts to recognize and prepare for changes that will affect both human and natural systems in the years to come.

Given its proximity to populated areas of northern Europe and its relatively modern, well-developed infrastructure, Svalbard is for many researchers one of the most accessible examples of a High Arctic landscape and climate. In combination with this accessibility, the long history of climate and earth systems research on Svalbard (e.g. Humlum, et al., 2003; Førland, et al., 2011) makes it an excellent location for work attempting to understand recent and ongoing changes in the Arctic climate. Linnévatnet, in western Spitsbergen, provides a high-resolution, annually varved sedimentary record which can serve as a proxy for past climate. Understanding this record and the

hydrological and sedimentary processes which contribute to it can provide insight into how the broader Arctic climate system has changed and is changing.

# Study Area

## Location

Svalbard is an archipelago located in the Barents Sea, roughly halfway between northern mainland Norway and the North Pole. The archipelago is composed of all of the islands between 74°N and 81°N latitude and 10°E and 35°E longitude, the largest of which is Spitsbergen. Linnévatnet lies in Linnédalen, a glaciated valley on the westernmost tip of the Nordenskiöldland region of the island, near the opening of Isfjorden to the Fram Strait and the Greenland Sea.


Figure 1.1: Map of Svalbard with Linnédalen's location highlighted by the red box (toposvalbard.npolar.no).


Figure 1.2: Map of Linnédalen, showing key features in the valley, including Linnébreen, Linnéelva, and Linnévatnet (toposvalbard.nploar.no)

# Linnédalen

Linnévatnet sits in Linnédalen, a NNW-SSE oriented valley approximately 14 km long from the top of Linnébreen at its head in the south to its outlet into Isfjorden in the north. Linnébreen has retreated rapidly since the Little Ice Age, exposing a large forefield of unconsolidated siliciclastic sediment. Linnéelva flows through the high moraine which marks the Little Ice Age extent of the glacier and continues approximately 5.5 km across the outwash plain to Linnévatnet. Sitting at 12 m above sea level, Linnévatnet is a glacially overdeepened basin approximately 4.7 km long (N-S) and 1.3 km wide, deglaciated around 12,300 yr BP (Snyder, et al., 1999). Open topography and a lack of vegetation around the lake allow wind to mix the water column and prevent stratification during the summer, ice-free months, keeping water temperatures below 4°C year-round (Bøyum and Kjensmo, 1978). Linnévatnet's southern half, proximal to the primary inflow and sediment source of Linnéelva, is shallow and divided into two sub-basins (east and west) by a mostly submerged ridge (Snyder, et al., 1999). Along the southern shore, Linnéelva flows into the 16 m deep east basin, while the 11 m deep west basin, separated by the submerged ridge, experiences less sedimentary and hydrological activity. The northern half of the lake consists of the single, 35 m deep main basin (Figure 3).

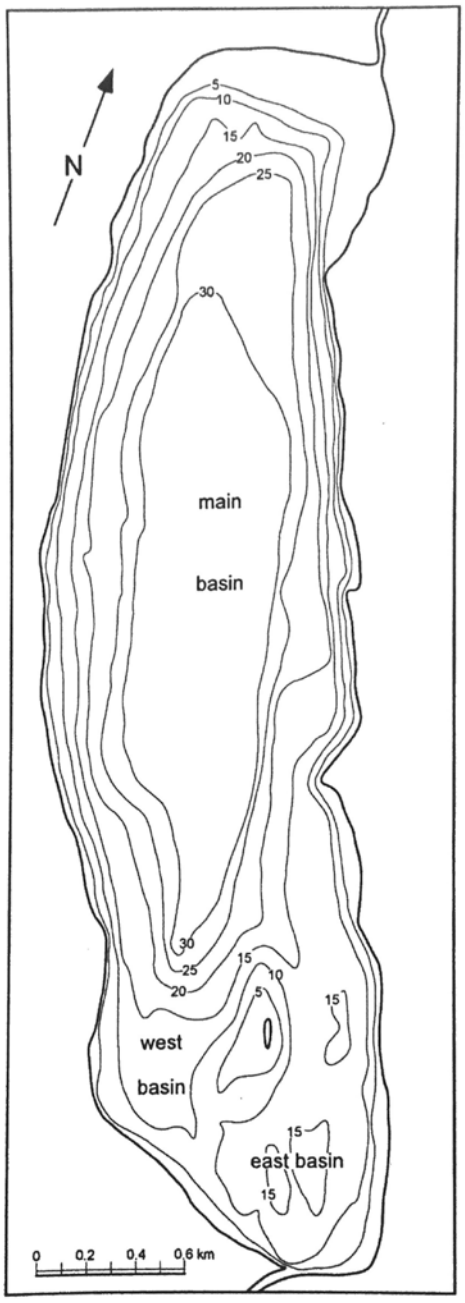


Figure 1.3: Bathymetric map of Linnévatnet with contours at 5 m intervals. (From Svendsen, et al., 1989)

## Glacial History and Surficial Geology

Svalbard, including Linnédalen, was covered during the Last Glacial Maximum by the Svalbard-Barents Sea ice sheet (Ingolfsson and Landvik, 2013). As the Late Weichselian ice sheet retreated, Linnédalen was deglaciated around 12,300 BP, as

recorded by radiocarbon dates on shells from the base of marine sediments in the valley (Mangerud and Svendsen, 1990). Those marine sediments, in places up to 8 m thick, were deposited when the isostatically depressed landscape was rapidly deglaciated, allowing the sea to fill the valley up to around 70 m above modern sea level, the marine limit (Mangerud and Svendsen, 1990). Isostatic rebound of the land surface outpaced sea level rise, leaving Linnévatnet isolated from the sea by 9600 BP (Svendsen and Mangerud, 1997). Since then, the sedimentary record in Linnévatnet has been recording changes in sedimentation and climate in the valley. This record indicates that the valley had no glaciers present from around 10,000 to around 4400 BP, when Linnébreen formed, due to combinations of warm climate and restricted precipitation (Svendsen and Mangerud, 1997). Glacier extent has fluctuated repeatedly since then, but the maximum extent was at the end of the Little Ice Age, in the late nineteenth century. The glacier's maximum extent is marked by a prominent Little Ice Age moraine (LIAM) (Svendsen and Mangerud, 1997). Today the valley floor is covered in a veneer of marine sediment (up to 70 m marine limit), till (especially above the LIAM), talus, and fluvial sediments.

# Bedrock Geology

Linnédalen rests on the West Spitsbergen Fold and Thrust Belt, a terrane of rocks uplifted during the Cretaceous rifting of the Arctic Ocean and then folded during Paleogene transpression as Greenland and Svalbard collided (Dallmann, 2015). The folding left the north-south striking rocks in Linnédalen dipping nearly vertically, meaning west-to-east travel across the valley carries one upwards through the local stratigraphy. Linnédalen is bounded to the west by highly metamorphosed argillaceous phyllites of the Precambrian Hekla Hoek Formation basement rock (Dallman, et al., 1992). The central portion of Linnédalen is composed of the plant fossil-rich quartzite of the Lower Carboniferous Orustdalen Formation. Linnédalen is bounded to the east by Upper Carboniferous carbonates and evaporates – primarily limestone, dolostone, gypsum, and anhydrite.

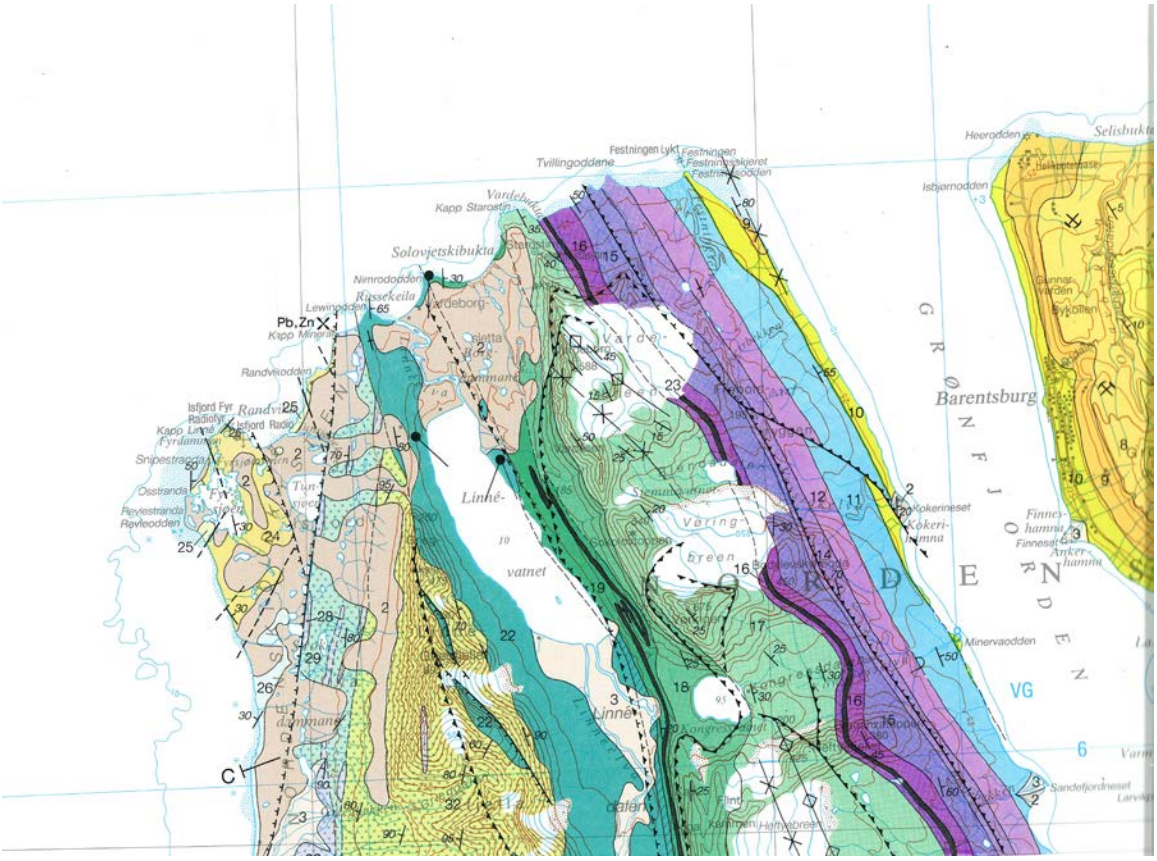


Figure 1.4: Geologic map of Linnédalen and surrounding area. The greens east of Linnévatnet are Carboniferous carbonates, the teal under and around Linnévatnet is Carboniferous quartzite, and the yellows west of Linnévatnet are Precambrian phyllites. From Dallman, et al. (1992).

# Climate

While Svalbard lies at high latitude, its mean annual temperature remained around -6˚ C for much of the 20th century, significantly warmer than other landmasses at similar latitude (Humlum, 2002). The mild climate is in part caused by the warm Atlantic waters of the West Spitsbergen Current, a branch of the warm, north-flowing Atlantic waters of the Norwegian current running along Svalbard's west coast (Førland, et al., 1997; Polyak and Jakobsson, 2011). This marine influence is more pronounced at sites like Linnédalen, in fjord troughs like Isfjorden (Isaksen, et al., 2016) and nearer to the coast, where precipitation can be more than two times higher than at central Spitsbergen sites such as Longyearbyen (Humlum, 2002). Winter temperatures can be especially volatile, meaning

precipitation can fall as rain or snow at any time of the year in Svalbard. Following the trend for “Arctic Amplification” of climate change (e.g. Serezze and Francis, 2011), temperatures and precipitation have both been increasing in recent decades on Svalbard, with annual temperature anomalies 1.7 to 2.5˚ C warmer from 2001-2015 than from 1971-2000 and especially high (3.4 to 4.6˚ C) positive temperature anomalies in the winter months (Isaksen, et al., 2016). These warming trends are expected to continue in the decades to come (Førland, et al., 2011). Warmer temperatures will mean earlier snow melt in the spring, a longer melt season, a conversely shorter snow accumulation season, and a higher proportion of rain to snow events, as warmer spring and fall temperatures will shift storms in the fall and spring “shoulder seasons” from snow to rain (Nowack and Hodson, 2013).

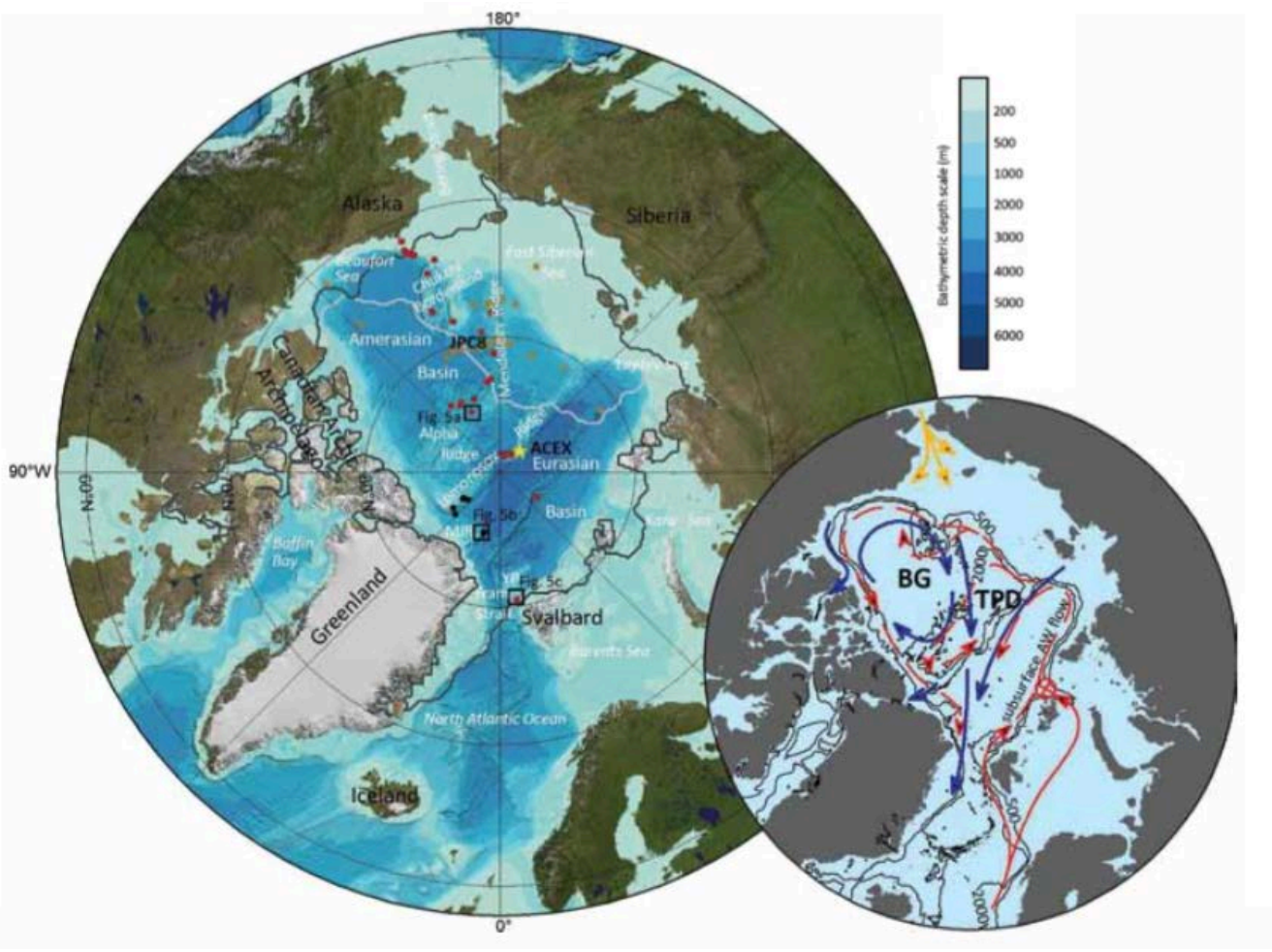


Figure 1.5: Bathymetric map of the Arctic Ocean with a diagram (inset) showing circulation patterns of warm (red) and cold (blue) waters, including the warm West Spitsbergen Current (Polyak and Jakobsson, 2011).

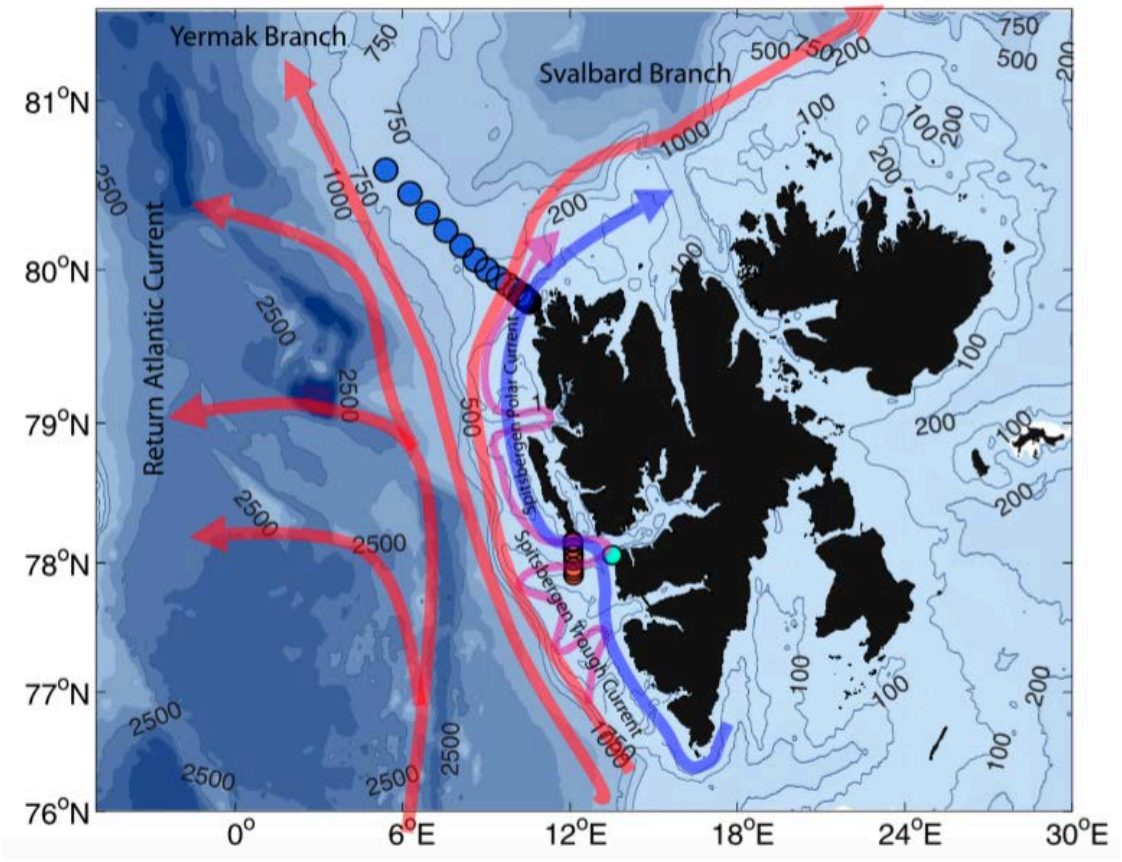


Figure 1.6: Detailed map of the dominant currents off the western coast of Spitsbergen. The red and purple arrows represent currents of warm Atlantic water which have a warming effect Svalbard, especially its westernmost regions (Nilsen, et al., 2016).

# Arctic Hydrology

Several elements of Svalbard's high Arctic environment provide hydrological and sedimentological conditions distinct from those controlling hydrology in other, more temperate regions. The permafrost which underlies much of Svalbard (Humlum and Sollid, 2003), including much of Linnédalen, is mostly impermeable and severely inhibits aquifers' water retention capabilities, instead diverting much of precipitation and meltwater to runoff. Linnédalen's recently deglaciated landscape and lack of vegetation leave a high proportion of the land surface covered in unconsolidated siliciclastic sediments. In combination with the high runoff caused by the impermeability of the permafrost, such conditions can lead to especially high sedimentation rates during melt or

precipitation events (Bird, et al., 2008). This is especially true when the active layer of seasonally freezing and thawing material at the land surface above permafrost is in its thawed, summer state.

In addition to the largely bare landscape and local topography, seasonal weather variations on Svalbard also have profound impacts on hydrology and sedimentation. Generally speaking, winter is marked by drastic decrease in sedimentation as freezing temperatures enclose the lake under ice and keep water frozen and stored in glacier ice and the snowpack (Zolitschka, et al., 2015). Without a source of liquid water, fluvial activity drops to zero or near zero, meaning the rivers are not transporting sediment (Lamoreaux and Gilbert, 2003). Meanwhile, the frozen lake surface also serves to block sediment which might be carried to the lake, for instance during occasional winter rainstorms (Førland, et al., 1997), and prevents wind from mixing the lake's waters, allowing the lake's waters to calm and fine sediment to settle out of suspension (Zolitschka, et al., 2015).

In spring, temperatures begin to rise above freezing and release water rapidly from the snowpack which built up over the winter. This nival flood often leads to a relatively short period of very high discharge in fluvial systems, during which the high energy of the system allows it to transport large amounts of sediment of a large average grain size (Woo and McCann, 1994). Discharge slowly tapers off over the course of the summer as the snowpack is depleted and glacial ice melt becomes a higher and higher proportion of the meltwater supply. Melt discharge is highest from June-August (Nowack and Hodson, 2013), but the warming climate on Svalbard (e.g. Isaksen, et al., 2016) will lead to the melt season starting earlier and continuing later into the year, leaving more time for melting and the increased rates of sedimentation it brings, with less time each year in the frozen, low-sedimentation state. Indeed, Frederiksen (2017) found that the number of days Linnévatnet is covered by ice each year has been decreasing since 2003, leaving the lake open to sediment deposition for a greater portion of the year. Later freeze dates in the fall have been the primary contributor to this loss in time of ice coverage, with some additional ice coverage time lost in the spring during years with prolonged periods of warmth and major rainfall events during the winter months. Such periods of

winter warmth and rain were interpreted to have thinned the ice, hastening ice melt in spring.

Another effect of the warming climate on Svalbard (Isaksen, et al., 2016) is the increased prevalence of fall rainstorms – the later onset of freezing conditions in fall (Frederiksen, 2017) results in autumn and winter precipitation falling more often as rain and less often as snow (Bintanja and Andry, 2017). These rainstorms can drive sedimentation in lakes at particularly high rates in fall (Retelle, et al., 2015; 2017), when nearly all of the active layer is thawed, whereas in spring much of the ground is still frozen, holding sediment in place.

# Arctic Lake Sedimentation

The distinctly seasonal variations in Arctic hydrology, particularly the contrasting high-discharge nival flood and winter, when the lake is calm and locked under ice, leave a distinctive pattern of varves in the sedimentary record of many Arctic lakes, including Linnévatnet. During the spring nival flood, the high-energy fluvial conditions carry a large amount of mostly coarse-grained sediment into the lake, with grain size decreasing throughout much of the summer as melt rates and flow rates decrease. This pattern of sedimentation, if undisturbed by rainstorms or slump events, generally results in a fairly thick, relatively coarse-grained graded bed representing the summer's sedimentation (Zolitschka, et al., 2015). Then, during the frozen winter months, the calm waters under the lake ice allow fine sediments suspended in the water column to settle out, forming a thinner, fine-grained "clay cap" winter layer on top of the thicker summer layer (Zolitschka, et al., 2015).

Clastic varves may preserve valuable meteorological records over both over both long-term and short-term timescales. Bird, et al. (2008) note that varves record a long-term record of summer temperature, spring melt intensity, and sedimentation rates, with a non-linear correlation between summer temperature and sedimentation rates in which a small increase in temperature can lead to a sudden increase in sedimentation. Hambley and Lamoreaux (2006) found that the cumulative melting degree days (a measure of the time and intensity of above-freezing atmospheric conditions throughout a year or season)

provided the best correlation to nival rhythmite thickness in a catchment with an unrestricted sediment supply. They also found that, in such a catchment, rain events late in the melt season produce distinct subannual layers in the sedimentary record. Cockburn and Lamoreaux (2008) suggest that short-term, high-intensity events such as large pulses of meltwater and late-season rainstorms are more important drivers of sedimentation rates than long-term factors like average summer or annual temperature. They suggest that analyses of the coarsest grains in a sample may be more appropriate than measurements of mean grain size for examination of deposition rates, given the correlation between coarse-grained sediment and these high-intensity sedimentation events. Chutko and Lamoreaux (2008) examine some thicker varves from high-sedimentation years and find that sub-annual events preserved in the sedimentary record correlate well with these high-intensity meteorological events. Given the increasing temperatures on Svalbard and their implications for the timing of the melt season and potentially increased prevalence of late-season rainstorms, it is important to better understand these high-intensity sedimentation events, and the increased role they may play in the annual sedimentation patterns. Retelle, et al. (2015; 2017) have already found that these events are playing a major and increasing role in sedimentation in Linnévatnet in recent years, and the recent research indicating that “shoulder season” rain events are becoming more common and more intense (Bintanja and Andry, 2017) suggests this trend for increased sedimentation will continue. Accounting for these major events and how they alter sedimentation patterns is essential if the high-quality varve record in Linnévatnet is to be used effectively as a long-term climate proxy.

# Previous Work and Study Goals

Over the past decade, Linnédalen has been the site of research performed by faculty and students in the Svalbard REU program funded by the U.S. National Science Foundation (NSF) and as part of courses run by the University Center in Svalbard (UNIS). Of particular relevance to this study, Walther (2015) used XRD analysis to examine the effects on sedimentation of high-intensity, late-season storm events, and McCabe (2016) used XRF analysis to examine the markers of these late-season storm events in the sedimentary record, with particular attention paid to geochemical evidence of their provenance. This study will use high-resolution grain size and XRF analyses to examine the links between specific weather events and associated markers in the sedimentary record from sediment traps deployed in Linnévatnet from July 2015 to July 2016.

# Chapter 2

# Methods

# Field Methods

## Moorings

This study utilizes twenty-four sediment traps placed on six moorings in Linnévatnet at the positions shown in Figure 4. Moorings C and D are in the eastern basin, in water around 15 m deep, near the inlet of Linnéelva and the lake's primary sediment source. Its proximity to the inlet makes the eastern basin the area of highest sedimentation in the lake (Svendsen and Mangerud, 1990), and moorings C and D are positioned in the basin to capture this high sedimentation signal. Mooring C experiences a higher sedimentation rate than mooring D by virtue of its more proximal position, relative to the inlet. Mooring D also receives some sediment input from the alluvial fan to its east. Mooring F is in the western basin, in water around 10 m deep. The western basin is separated from the eastern basin by a bathymetric ridge, and is thus separated from the primary sediment source of Linnéelva. Mooring E is located on the bathymetric ridge separating the eastern and western basins, in water only about 5 m deep. Moorings E and F experience much lower rates of sedimentation than Moorings C and D. Moorings H and G are in the deep main basin at the northern end of the lake. Mooring H occasionally receives additional sediment from an alluvial fan to its east (McCabe, 2016) while Mooring G, the most proximal of the moorings, is designed to record a model of the sedimentation in the lake as a whole, with no nearby sediment source which might have a disproportionate influence on the sediment traps attached to the mooring.

## Sediment Traps

The sediment traps affixed to the moorings consist of a 12.1 cm-diameter funnel topped by a baffle of 1 $cm^2$ plastic grid. Sediment deposited in the funnel accumulates in a receiving tube affixed to the bottom of the funnel with electrical tape. The trap is attached to the mooring line with an L-shaped bracket and cable ties. The bracket keeps the trap upright and stable in the water column. The funnel, with a diameter greater than that of the receiving tube it feeds, amplifies the sedimentary signal (Asper, 1987). Sedimentation rates with the funnel are about 8 times those on the lakebed nearby. The

plastic grid of the baffle disrupts laminar flow in the water column, allowing sediment to settle out of suspension, while also preventing turbulence in the funnel and receiving tube which might disturb already-deposited sediment. An example of the sediment traps can be seen in Figure 5.

These traps are arranged along the vertical lines of the moorings as seen in Figure 6, weighted down at the bottom with a large rock and tied at the top to a buoy floating around 1 m below the lake's surface so that it is not encased and dragged by winter lake ice. The lowermost trap is placed 1 m above the rock at the bottom of the mooring, and subsequent traps are spaced from 3 m above the trap below.

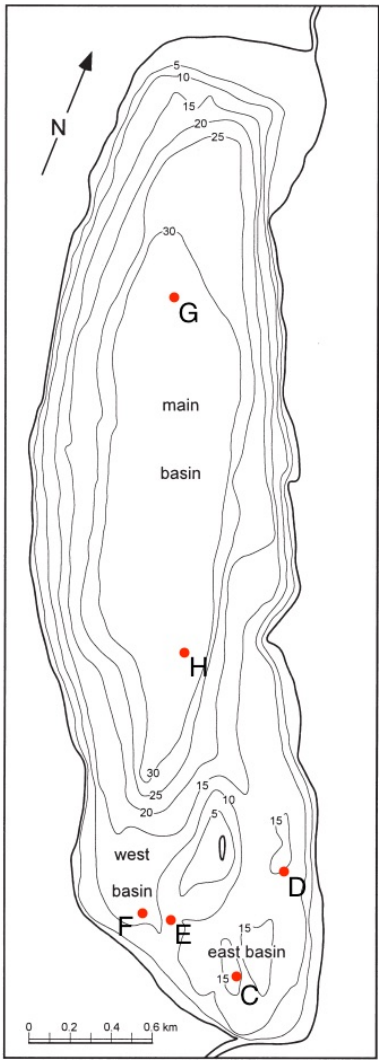


Figure 2.1: Bathymetric map of Linnévatnet with the locations of mooring sites in the lake marked. Modified after Svendsen, et al. (1989).

Figure 2.2: A sediment trap after removal from the mooring line

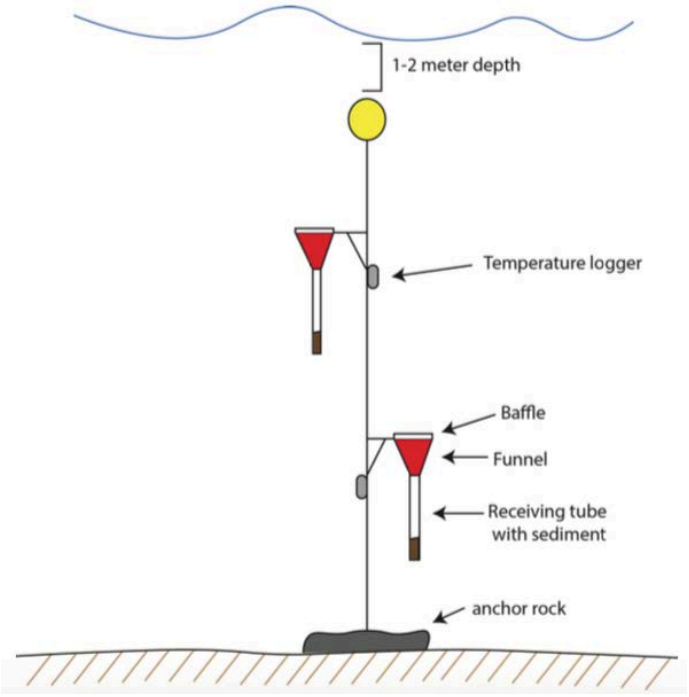


Figure 2.3: Diagram of the arrangement of sediment traps on mooring lines (McCabe, 2016, after Arnold, 2009).

## Sediment Trap Collection

The moorings were deployed in Linnévatnet from July 2015 until July 2016. During field work, the sediment traps were collected by boating to their location in the lake and hauling the moorings up into the boat by hand, removing each sediment trap and keeping it vertical as it emerged from the water. The sediment-capturing tubes were then removed from the funnels and capped for transportation to the group's field lodging. There, Zorbitrol® Plus Superabsorbent Polymer was added to the water which filled the space in the receiving tube above the sediment, and the tubes were re-capped and sealed with tape.

Zorbitrol® Plus Superabsorbent Polymer is a sodium polyacrylate powder which readily absorbs large amounts of water, forming a gel to preserve and stabilize the sediment-water interface and underlying stratigraphy during transportation (Tomkins, et al., 2008). During transportation from the group's field lodging at Isfjord Radio back to Longyearbyen, the samples were agitated enough that some exhibited dewatering and

related compaction of the sediment in the receiving tubes. The original Zorbitrol® gel was removed from the affected samples and replaced to again stabilize the sediment for travel from Svalbard to the USA.

## Intervalometer

The intervalometer is a sediment calibration instrument deployed in the lake at Mooring C during the same period in which the sediment traps were deployed. It records the timing of sediment deposition at 30 minute intervals using a vertical column of LEDs facing light sensors across a receiving tube fed by a funnel and baffle system like those in the sediment traps. LEDs turn off as accumulating sediment blocks their light from reaching the corresponding light sensor, and a corresponding increase in voltage is recorded. A HOBO logger records the voltage in the instrument every 30 minutes, providing a record of the timing of sediment deposition.

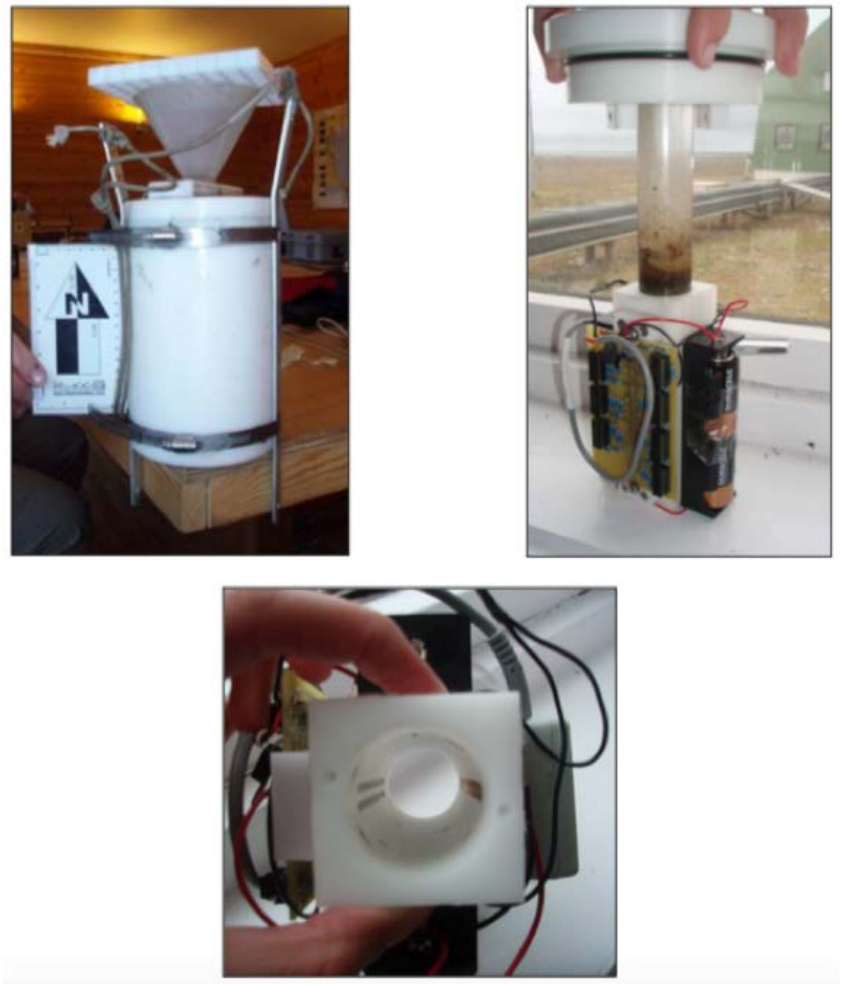

Figure 2.4: Photographs showing the intervalometer. The instrument consists of a receiving tube attached to a baffle-covered funnel, much like the sediment traps. The receiving tube is situated between LEDs and light detectors which record the timing of sediment deposition as the receiving tube fills and blocks the LEDs' light (Arnold, 2009).

## Time Lapse Photography

Cameras overlooking Linnébreen and the southern end of Linnévatnet, including the inlet of Linnéelva, were programmed to take two photographs each day. While they do not provide data during the dark period from late October to February, they provide valuable data for the spring, summer, and fall months. The photographs allow for visual monitoring of the timing of snow melt, ice melt on the lake, flow in Linnéelva, and sediment plumes in the lake.

# Meteorological Data

Meteorological conditions in Linnédalen were recorded using an ONSET HOBO U30 weather station near the southern shore of the lake. The station has been recording data in the valley since the 2003-2004 sediment year and logs air temperature, ground temperature, relative humidity, precipitation, wind direction, and incoming solar radiation at 30 minute intervals. The solar radiation, wind direction, and precipitation data logs stop on 12 March 2016. The stoppage occurred at 10:00 AM for solar radiation and wind direction and at 10:30 AM for precipitation. The wind speed, air temperature, and ground temperature logs continue through 22 July 2016, when the data logs were downloaded.

These data are supplemented by air temperature data from sensors in five other nearby locations: Little Ice Age cirque, Little Ice Age Moraine, mid-glacier, upper glacier, and Isfjord Radio. The data not recorded on the main weather station after the March equipment failure can be partially accounted for using meteorological data from the weather stations at Isfjord Radio and the Longyearbyen Airport (LYR). Isfjord Radio sits just west of the mouth of Linnédalen while LYR is approximately 80 km east of the study site, up-fjord in Isfjorden. These sites can have localized weather patterns very different from those in Linnédalen, but the data can be used to learn about broad regional weather events. Data from these weather stations were downloaded from the Norwegian Meteorological Institute (eklima.met.no).

Figure 2.5: The main weather station near the southern shore of Linnévatnet.

# Laboratory Methods

## Receiving Tube Preparation

After transportation from Svalbard to Bates College, the receiving tube from the bottom-most sediment trap on each mooring was prepared for magnetic susceptibility, grain size, and geochemical composition analyses. Peter Beach, the shop mechanic at Bates College, used an apparatus of his own design and construction to score two lines opposite one another on the plastic receiving tubes. The plastic was scored without

penetrating all the way through to the sediment inside in order to prevent contamination from the saw blade or chips of plastic, which might affect the analyses to be performed later. Once scored, the tubes were split lengthwise into two halves by prying with a flathead screwdriver. Once the plastic tubes were split, the sediment core inside was split into halves corresponding to the halves of the tube using a piece of aluminum siding. The receiving tubes were logged and photographed. The half with the smoothest, least disturbed surface was wrapped in plastic, used for non-destructive analyses, and saved as an archive half. The lower quality half was designated the working half and used for the destructive grain size analysis.

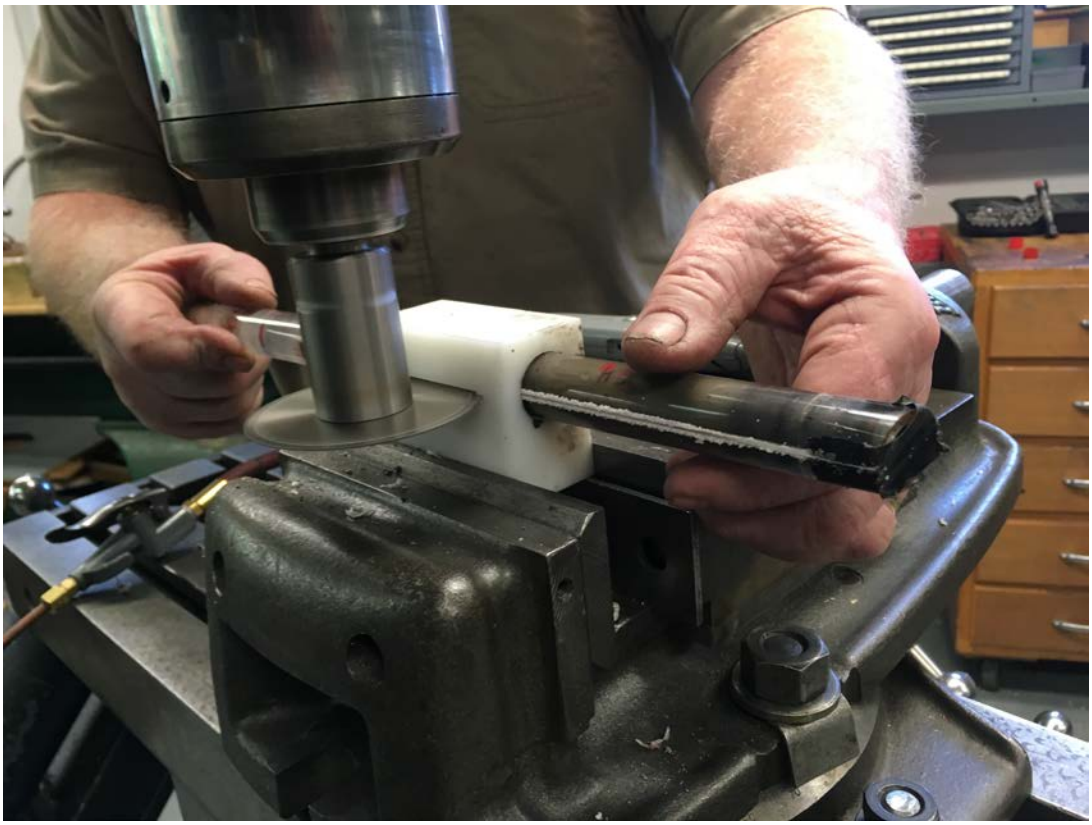

Figure 2.6: The receiving tube from sediment trap C4 being scored by Bates College shop mechanic Peter Beach in the apparatus he designed and built.

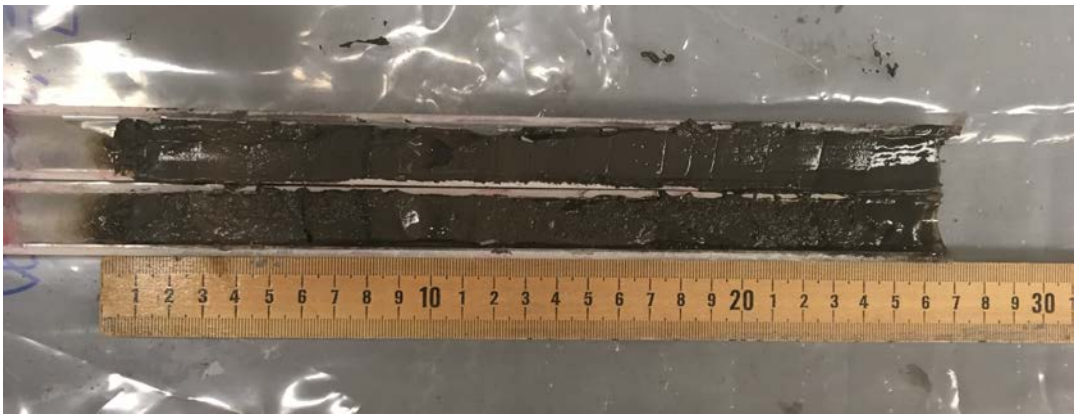

Figure 2.7: The receiving tube from sediment trap C4 after being scored and split.

The working halves of the receiving tubes were continuously sampled downcore at 0.5 cm intervals and prepared after the procedure outlined by Arnold (2009). Each 0.5-cm slice from the sediment core was placed in a 50 mL centrifuge tube, to which 1 mL of concentrated (30%) hydrogen peroxide ($H_2O_2$) was added, along with enough deionized water to cover the sample, if it was not covered by the $H_2O_2$. The samples stayed in the $H_2O_2$ for at least 24 hours to remove any organic matter. The centrifuge tubes were left uncapped during this time to allow for the escape of gas produced as the $H_2O_2$ reacted with the organic matter. After at least 24 hours had passed, 20 mL of deionized water and 17 mL of 0.7 g/L sodium metaphosphate dispersant were added to each sample. A Vortex Genie 2 was used to agitate each sample before it was added to the sample chamber of the Beckman Coulter Laser Particle Size Analyzer (LPSA).

In the LPSA, the sediment from the sample is suspended in an aqueous solution and pumped through an analysis chamber where a laser shines through the sample. The light diffracted around individual particles is measured by a series of light detectors, and grain size is calculated for each particle based on the diffraction pattern. The LPSA provides a statistical summary of the grain size distribution for each sample. The LPSA analyzed each sample three times. Unless it produced an error, data from the third trial were used in order to give the sonic dismembrator agitating the sample the greatest possible chance to break apart any aggregated particles. Mean, median, and $90^{th}$ percentile grain size were recorded for each sample.

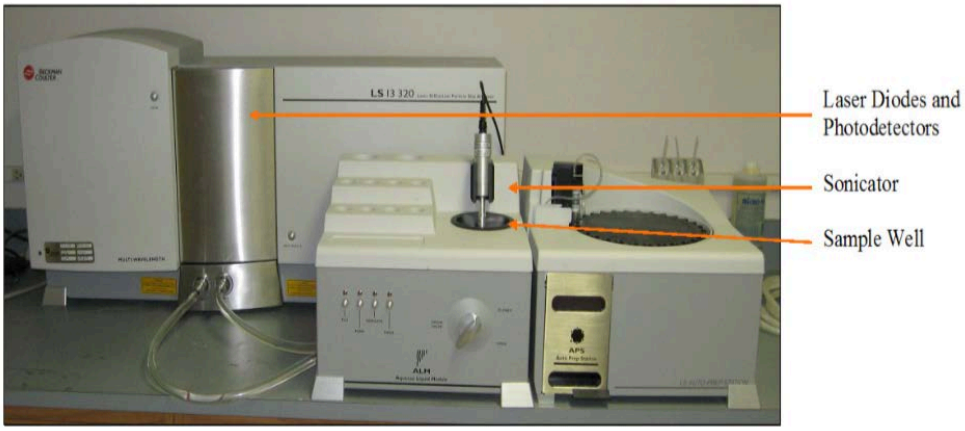


Figure 2.8: Image showing the Beckman Coulter LPSA with some important components labeled (Walther, 2015, after Arnold, 2009).

# ITRAX XRF Analyses

X-ray fluorescence (XRF) analyses were used to examine the geochemical composition of each sediment trap downcore. Such analyses can be useful in studies of lacustrine sediments by revealing variability in sediment source and deposition mechanism (Cuven, et al., 2011; Shanahan, et al., 2008). The Cox ITRAX XRF Core Scanner at the Ronald B. Gilmore XRF Laboratory at the University of Massachusetts, Amherst was used for these analyses.

The archive halves of the receiving tubes were each scanned twice, from top to bottom. The first scan produced an RGB image of the cores, a radiograph (50 kV, 40 mA, 700 ms exposure time), and a laser topographic profile of the core's surface (Croudace, 2006). The cores were then re-loaded into the instrument and scanned a second time, this time using XRF. Start and end points for this XRF scan were chosen on the RGB image from the first scan so that only the sediment cores (and not empty sections of the receiving tubes) were being scanned. A molybdenum (Mo) tube was used to generate X-rays with a voltage of 30 kW and current of 55 mA. XRF measurements of 500 micron increments of the cores were recorded with 10 second exposures, while the topographic profile from the first scan was used to keep the ITRAX XRF detector a constant height above the sample's surface (Croudace, et al., 2006). The scans produced downcore profiles showing the elemental makeup of the sediment in each trap.


Figure 2.9: The Cox ITRAX XRF Core Scanner at the Ronald B. Gilmore XRF Laboratory at the University of Massachusetts, Amherst.

## X-Ray Diffraction

After identifying key zones of sediment in trap C4 based on the grain size and XRF profiles, segments of sediment between 0.5 and 2.0 cm thick were removed for X-ray diffraction testing of their mineral content. Trap C4 was used for this analysis because it received the most sediment and thus had the highest-resolution sedimentary record. Samples were taken of the sediment between the depths of 0 and 1 cm, 3.5 and 4.5 cm, 11.5 and 12 cm, 18.5 and 19.5 cm, and 24 and 26 cm. Each sample was dried for more than 48 hours at 60° C in a drying oven, then crushed using a mortar and pestle in order to break apart clustered sediment grains. Each sample was analyzed with the Rigaku B X-ray diffractometer at Bates College, and the resulting diffractograms were analyzed using KS Analytical Systems' Jade software to determine mineral content. While the XRD analysis is useful for determining what minerals are present in the sample, there is a high degree of uncertainty associated with the stated proportions of each mineral in the samples. The presented proportions of mineral content should be taken as no more than approximate.

# Chapter 3

# Results

# Weather

Weather data were collected from July 24, 2015 to July 19, 2016 at the weather station near the south shore of Linnévatnet. Rain, wind direction, and solar radiation detectors stopped working on 12 March 2016. Air temperature, ground temperature, and relative humidity detectors continued to run for the entire year. Presented below in Figure 3.1 are the records of precipitation and air temperature for the entire year, followed by detailed records for significant meteorological events during the year (Figures 3.2-3.4).

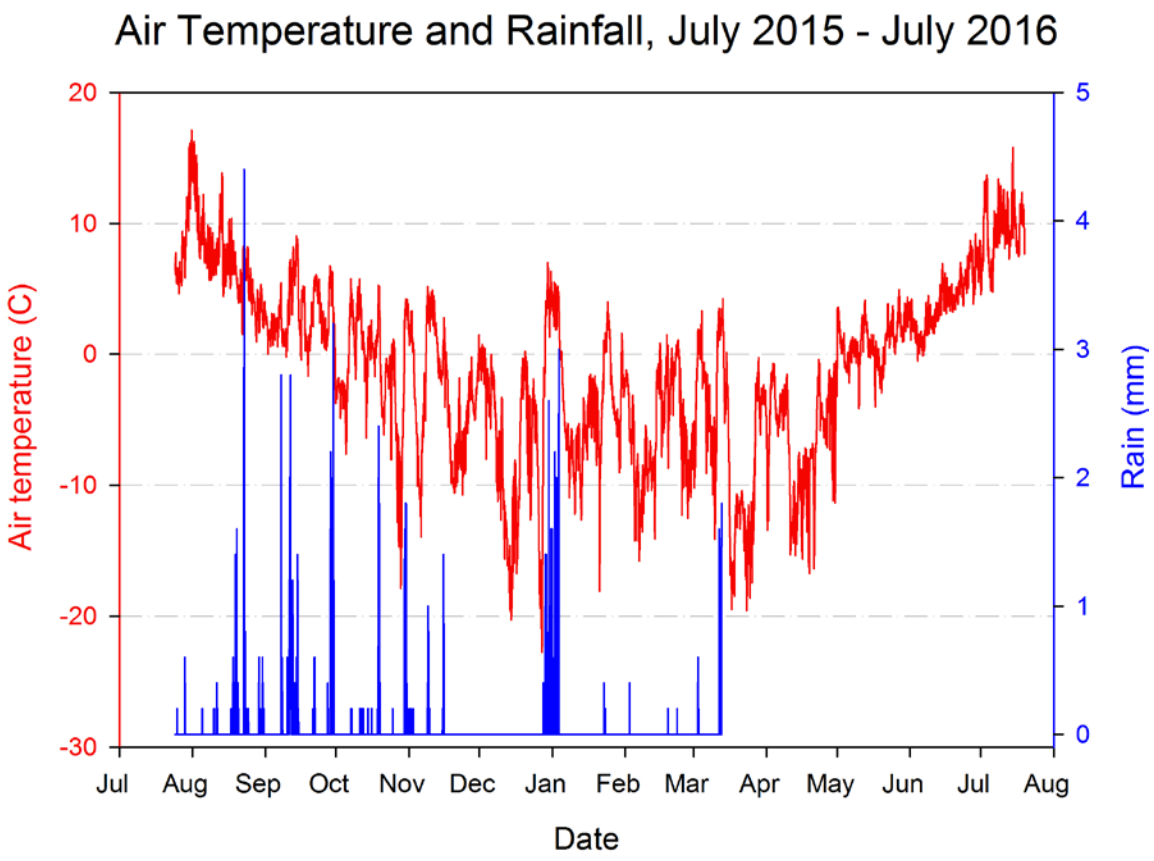


Figure 3.1: Air temperature and rainfall totals per 30-minute interval for the year of July 2015 to July 2016. The precipitation logger stopped at 10:30 am on 12 March 2016.

From September 11-12, 2015, 49.2 mm of rain fell at the weather station in 48 hours. This storm event occurs at the same time as a large depositional event shown by the intervalometer (shown later in this section). A detailed graph of rainfall and air temperature over time is shown below (Figure 3.2) for the period of this storm event. The

storm featured prolonged rainfall, with several periods of sustained high intensity. Note that the storm was also preceded and followed by small, sporadic bursts of rainfall.

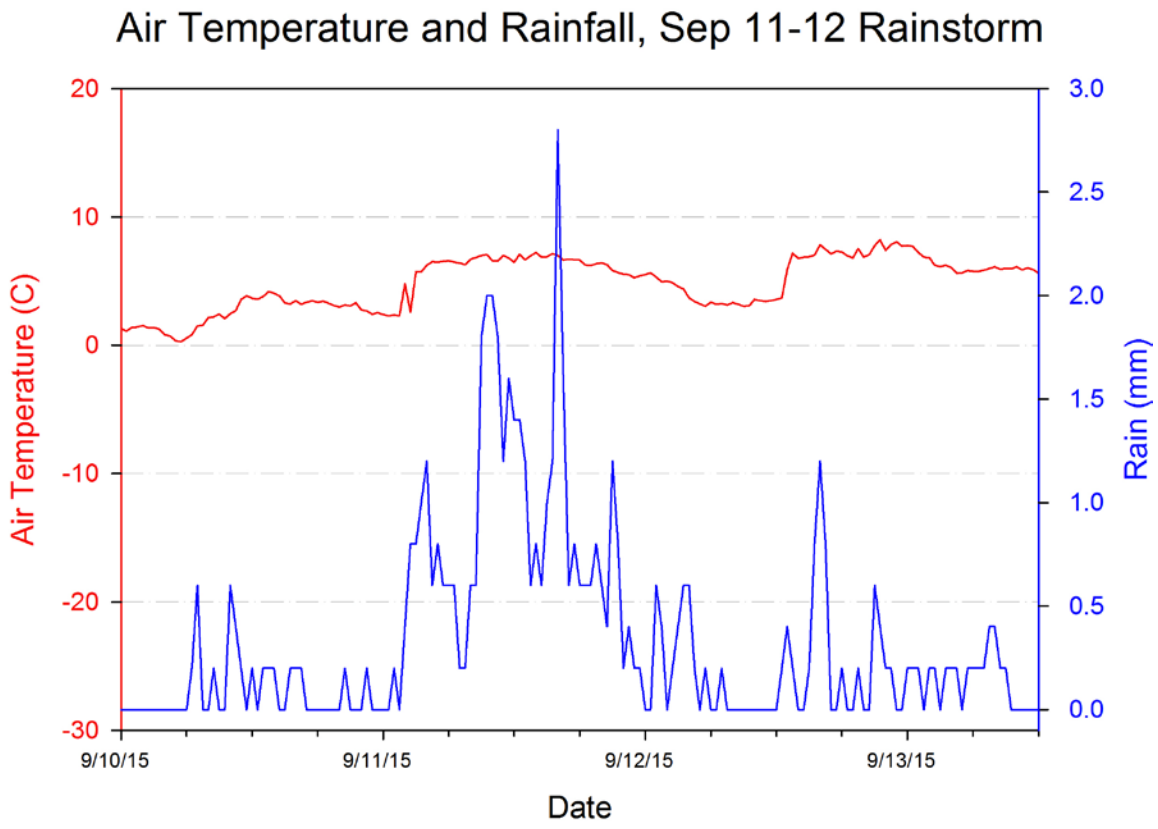


Figure 3.2: Detail of rainfall over time for the rainstorm of September 11-12, 2015.

Below are a graph of rainfall and temperature (Figure 3.3) and a graph of air, ground and stream temperature (Figure 3.4) during late December 2015 and early January 2016. Models of annually varved lake sediments usually have the lake and surrounding landscape frozen over, with no sediment input during winter. These data, combined with the intervalometer record (later in this section) showing deposition during the same period indicate that the assumption did not hold true in the winter of 2015-2016. Rather, air temperature was consistently above 0° C for nearly six days. Ground temperature at 50 cm depth reached a maximum of -0.004° C and remained near 0° C for several days, meaning the surface was likely thawed, leaving sediment free to be transported. 107.2 mm of rain fell over a seven-day period and stream temperature rose above 0° C, indicating flowing water.

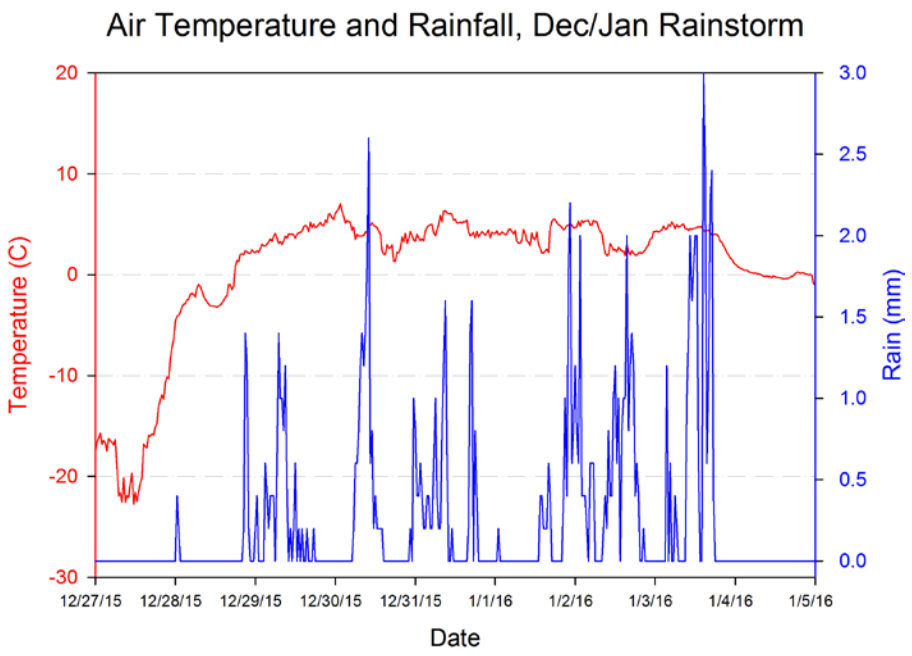


Figure 3.3: Rainfall and air temperature per 30-minute interval during the December-January rain event. During the period shown, a total of 107.2 mm of rain fell.

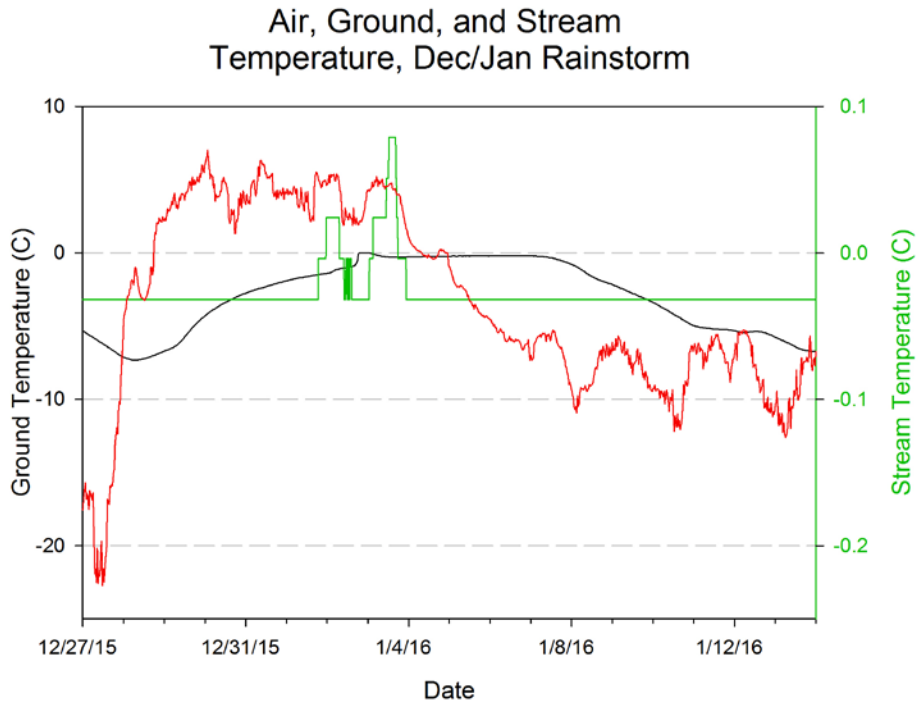


Figure 3.4: Air, ground, and stream temperatures during and after the December-January rain event. During the period of warm air temperatures and rainfall, ground temperature at 50 cm depth nearly reached 0° C, and stream temperature twice exceeded 0° C.

# Intervalometer

The intervalometer recorded sediment deposition at Mooring C from July 19, 2015 to July 22, 2016 in 30-minute intervals. The record has been divided into five distinct events, E1-E5, representing sedimentation associated with distinct events or processes throughout the time of deployment. E1 is a series of small, distinct depositional events occurring from deployment in July through early September, representing pulses of meltwater from Linnébreen or relatively small precipitation events. Nearly 70% of the sedimentation for the year came on September 11$^{th}$ and 12$^{th}$, 2015, corresponding with a large rainstorm. This short, intense period of deposition is denoted as E2. E3 is a small pulse of sediment recorded during the warm, rainy week in early January 2016. The nival flood, the onset of sedimentation during the spring melt season, is denoted E4. E5 is the remainder of sedimentation fo the year, occurring in summer, when sedimentation would be primarily due to small rain events or pulses of meltwater from Linnébreen, as in E1. These events are distinguished below on a graph of both sedimentation and rainfall for the duration of the intervalometer's deployment (Figure 3.5). Detailed graphs of E2 and E3 sedimentation are also provided (Figures 3.6 and 3.7, respectively)

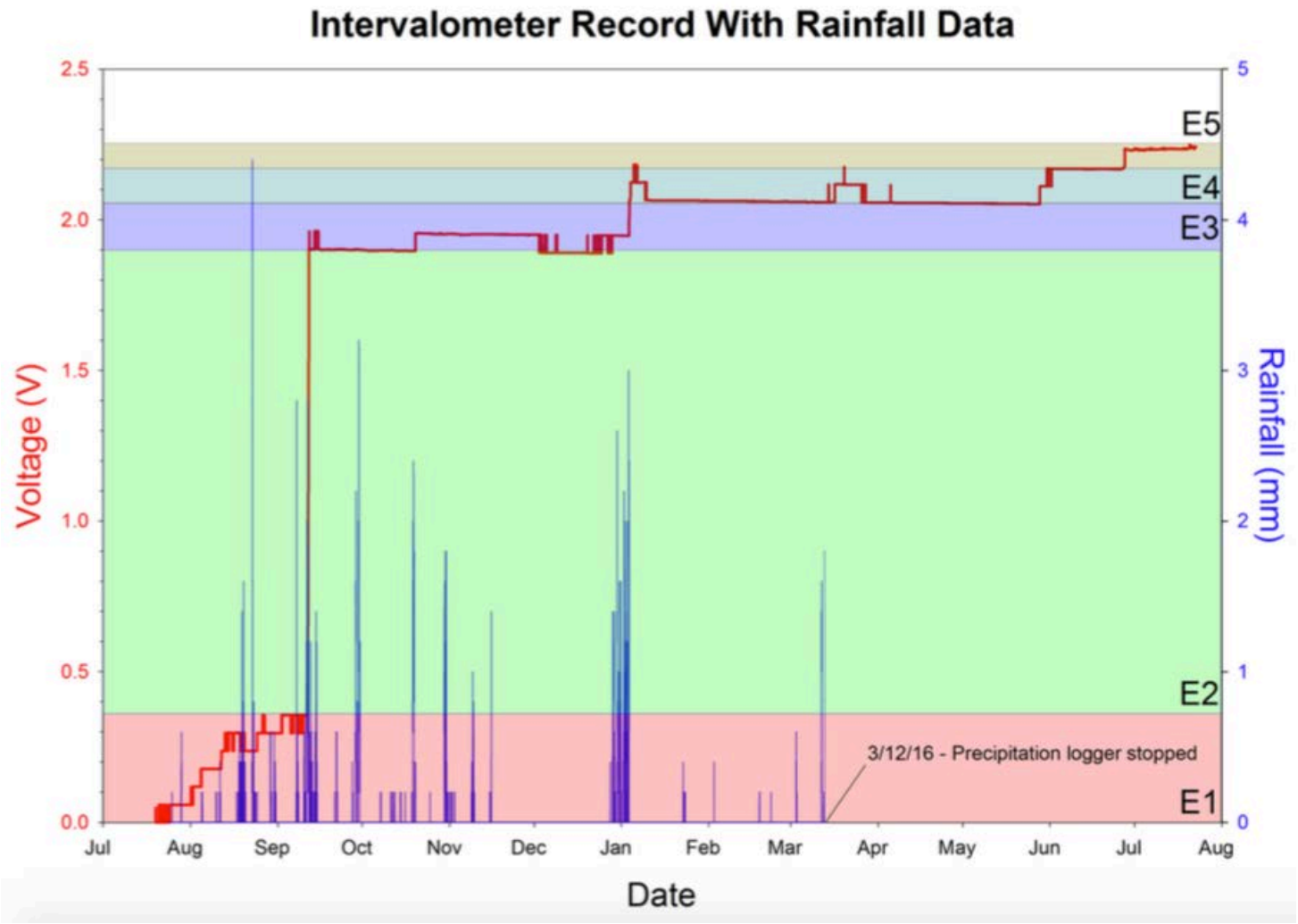


Figure 3.5: Intervalometer record for the entire duration of its deployment, 7/19/15 – 7/22/16, with rainfall data through 3/12/16, when the precipitation logger failed. The record is divided for reference into five distinct events, E1-E5, marked here by colored boxes.

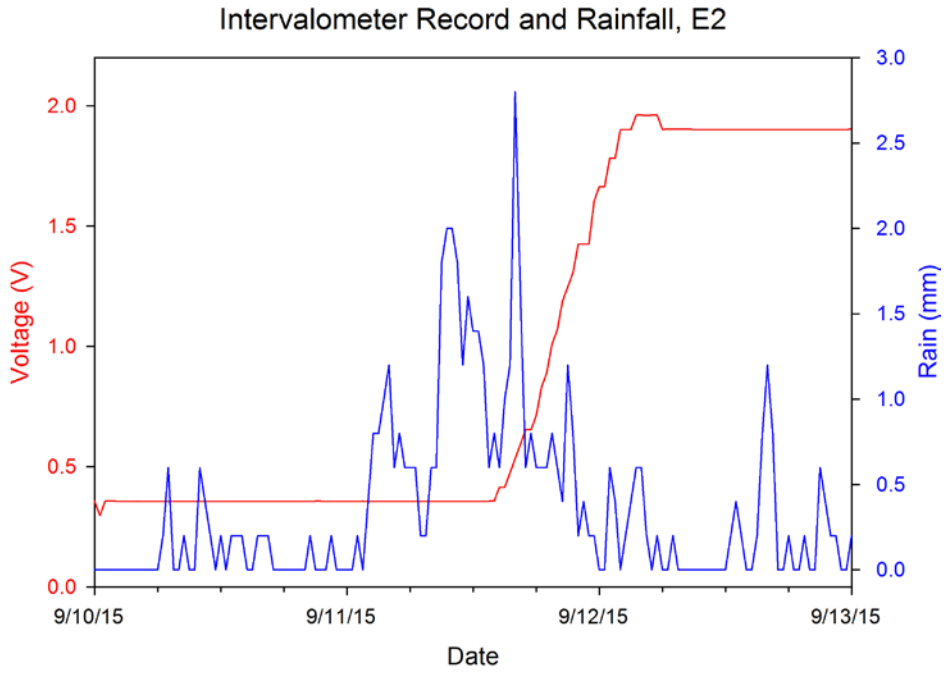


Figure 3.6: The record of sedimentation and precipitation for E2. The increase in voltage, representing about 70% of the year's sedimentation, occurred in a 17-hour period, from 1:30 pm on 9/11 to 6:30 am on 9/12.

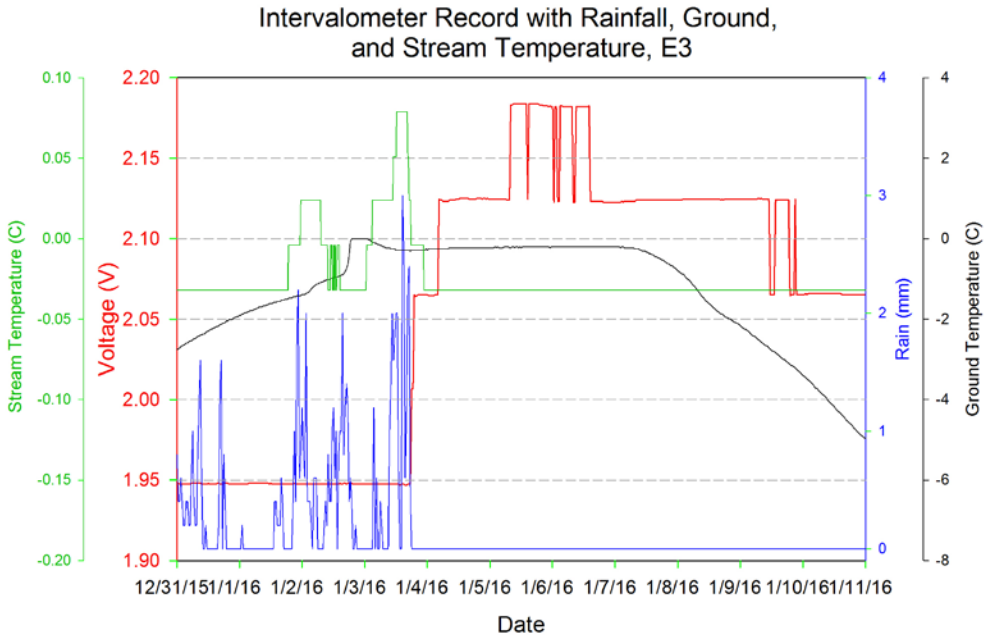


Figure 3.7: Intervalometer record showing sedimentation, rainfall, ground temperature, and stream temperature during E3. Sedimentation followed soon after the stream and ground temperatures rose to or above freezing during some of the most intense rainfall.

## Grain Size Analyses

Grain size analyses on the Coulter LPSA yielded the downcore grain size profiles with median, mean, and d90 grain size for the cores of the lowermost sediment trap on each mooring. They are shown side-by-side in Figure 3.8, arranged from most proximal to most distal along the transect from Mooring C to Mooring H, with profiles from the cores on Moorings E and F at the far right. The sediment signatures of E1-E5 are correlated along the transect in Figure 3.9, using only the median grain size profiles. Profiles from E and F are not included in this figure, as their position in the western basin shielded them from E2 and E3 sedimentation by the bathymetric ridge on which Mooring E sits.

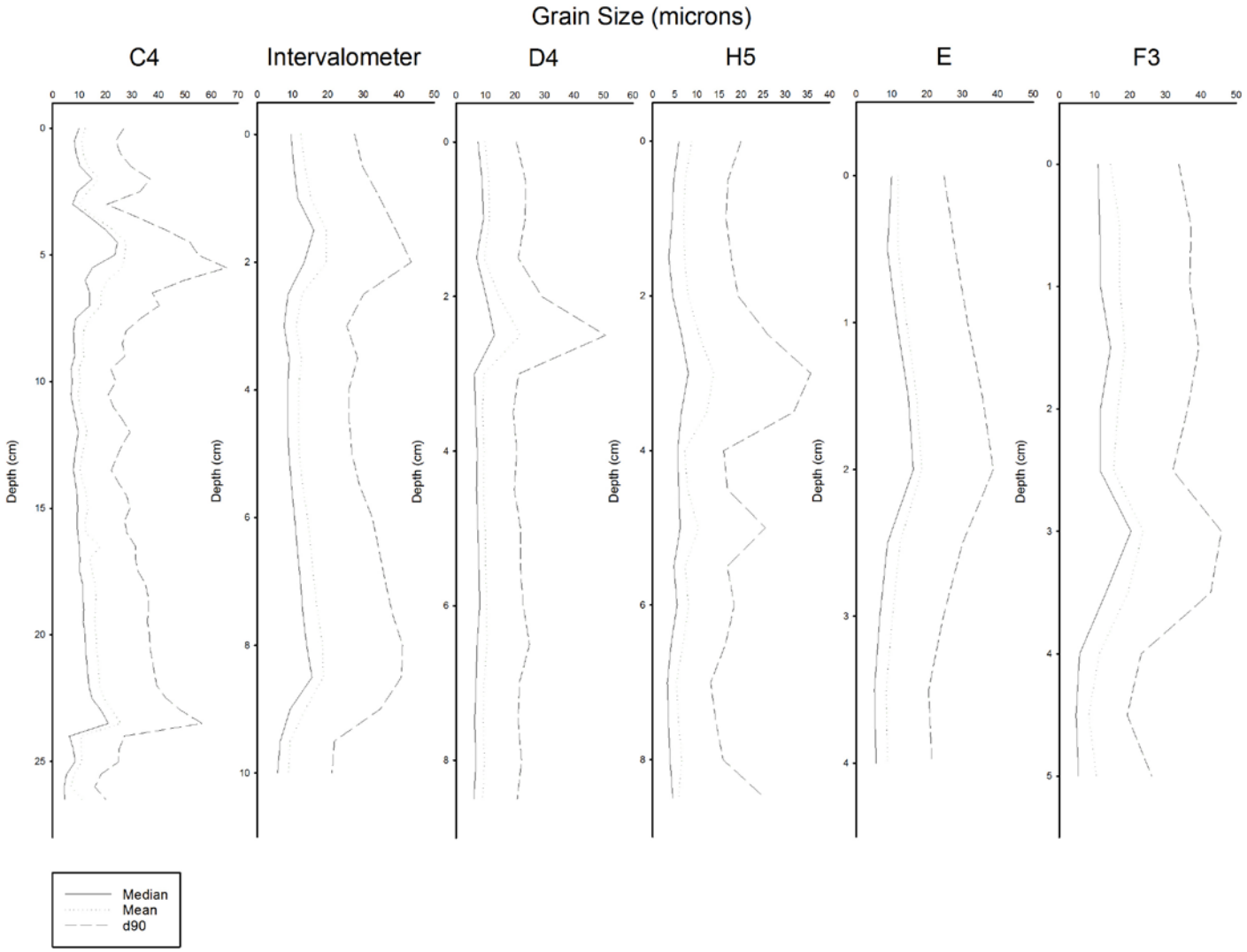


Figure 3.8: Median, mean, and d90 grain sizes from the sediment traps in Linnévatnet, presented side by side

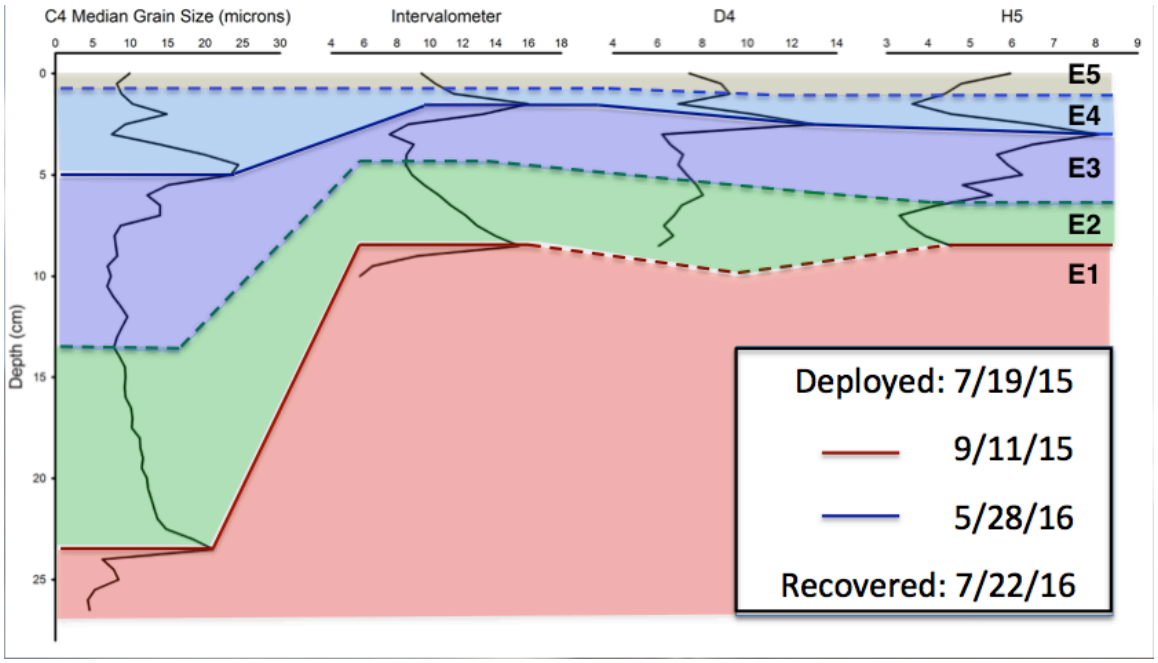


Figure 3.9: Median grain size profiles, to scale, from the sediment traps along the transect from Mooring C to Mooring H, with the sediment signatures of E1-E5 marked.

Along the transect from C to H, all of the traps show a sharply defined zone of increased grain size near the top of the core, immediately above some of the finest-grained sediment in each core. These are the coarse-grained sedimentary signatures of the nival flood, E4, immediately overlying the fine sediment of E3. C4, the Intervalometer, and H5 also show a zone of coarse grain size at or near the bottom of the core, interpreted as the lower boundary of E2. D4 has no such coarse-grained signature near its bottom, which is taken as an indication that E2 sedimentation varied spatially across the lake. The boundary between E2 and E3 is inferred, as the fine-grained upper portion of E2 tends to blend with the fine-grained E3. In F3 and E, only one zone of large grain size is present in each core, a signature of E4. The grain size maximum is around halfway down the core in each case. The fine grains at the bottom and top of most cores are taken as the signatures of E1 an E5, respectively.

Minimum median grain size remains consistent throughout all of the sediment traps, always around 5-10 microns. Maximum median grain size, however, varies somewhat more. In C4, D4, and F3, maximum median grain size is around 22-27 microns, while it is only around 16-18 microns in E, H5, and the Intervalometer. In

general, the coarsest grain sizes are found at the most proximal moorings, and these moorings tend to have the thickest packages of sediment. The finest grains are found at moorings farther from major inlets or sources of sediment. The traps on these moorings tend to have the thinnest packages of sediment.

## ITRAX XRF Profiles

ITRAX XRF analyses of the sediment trap cores yielded downcore elemental composition data and the ability to analyze how elements co-vary within a core. In the attached Figures 3.10-3.15 are charts showing these downcore profiles for Zr, Ca, K, and Fe for each sediment trap. These elements were chosen for closer examination due to their strong relationships with trends or particular markers in the grain size profiles. The elemental composition profiles are presented along with a downcore median grain size profile, the optical core scan from the ITRAX scanner, and the best estimates of date ranges for deposition of certain segments of sediment, based on the intervalometer and weather records. In traps D4, E, F3, and the intervalometer core, compaction during transportation of the traps and surface irregularities made parts of the core unreadable to the ITRAX scanner which did yield enough sediment for grain size analyses. Thus, especially near the bottoms of cores, there are places where the grain size profile is several cm longer than the ITRAX XRF profiles. Superimposed on all of the profiles are boxes categorizing the sediment by depositional event, E1-E5. Signatures for E2 and E3 were not present in traps E and F3. Where possible, sharp changes in grain size or one or more elemental profiles were used to mark the boundaries of these sediment categorizations. In places where such sharp changes were not present, smaller changes in grain sie or chemical composition were used to infer boundaries. Where these inferences were made based on subtle changes in sediment character, the positioning of these boundaries has a high degree of uncertainty.

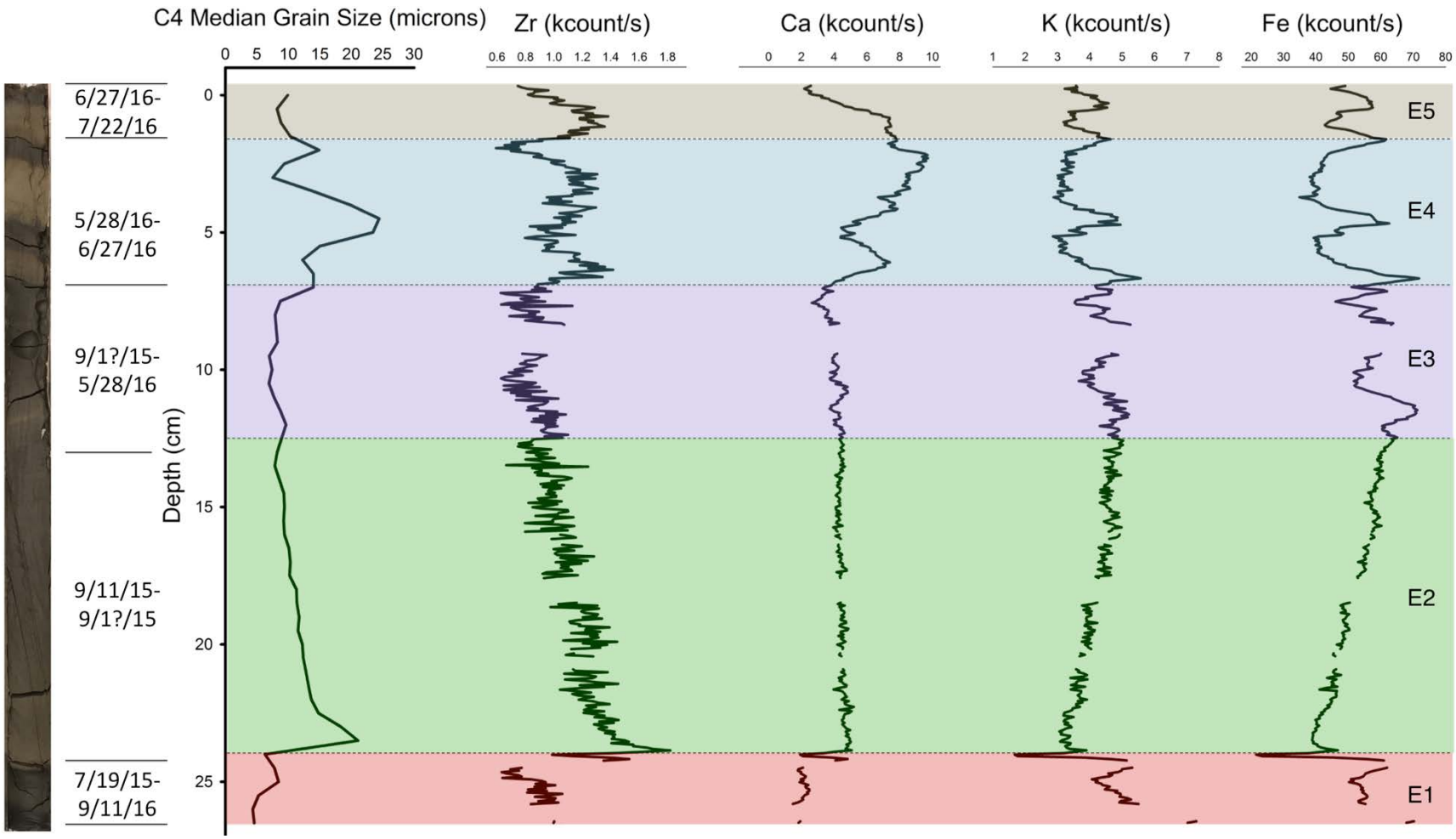


Figure 3.10: ITRAX elemental profiles from trap C4, with E1-E5 marked, the best known corresponding dates, and an image of the core.

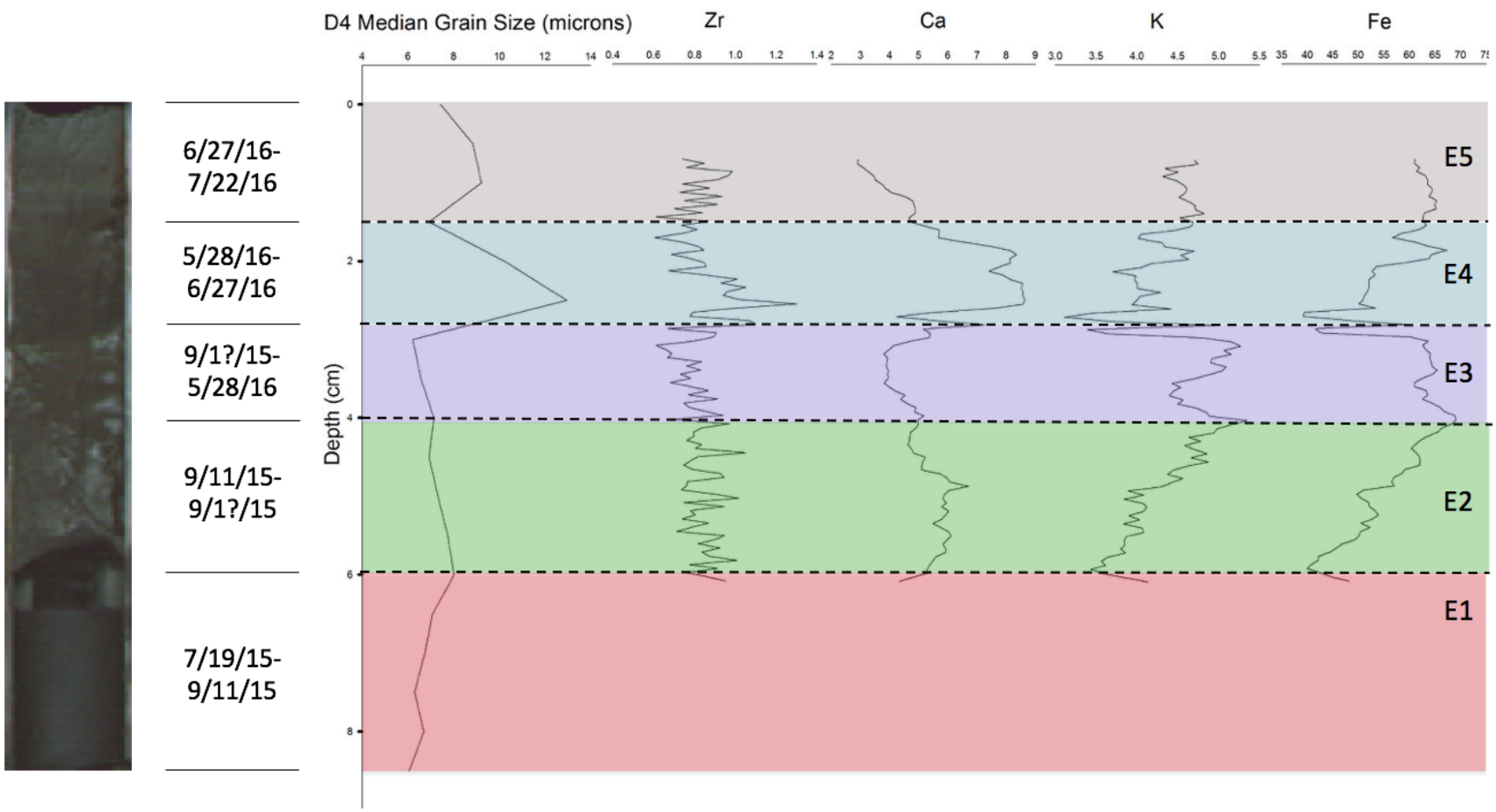


Figure 3.11: ITRAX elemental profiles from trap D4, with E1-E5 marked, the best known corresponding dates, and an image of the core.

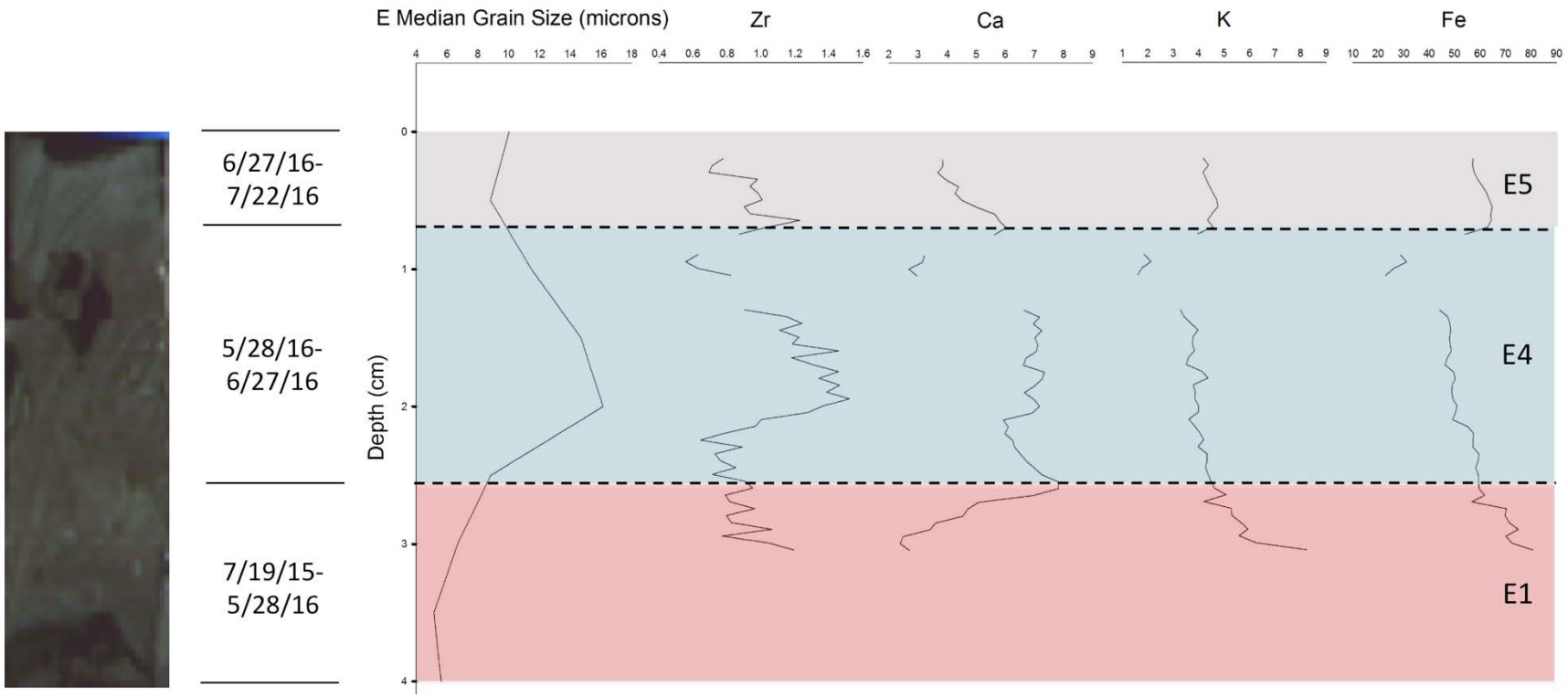


Figure 3.12: ITRAX elemental profiles from trap E, with E1 and E4-E5 marked. Sediment signatures from E2 and E3 were not present in the core from E. Provided at left are the best known corresponding dates and an image of the core.

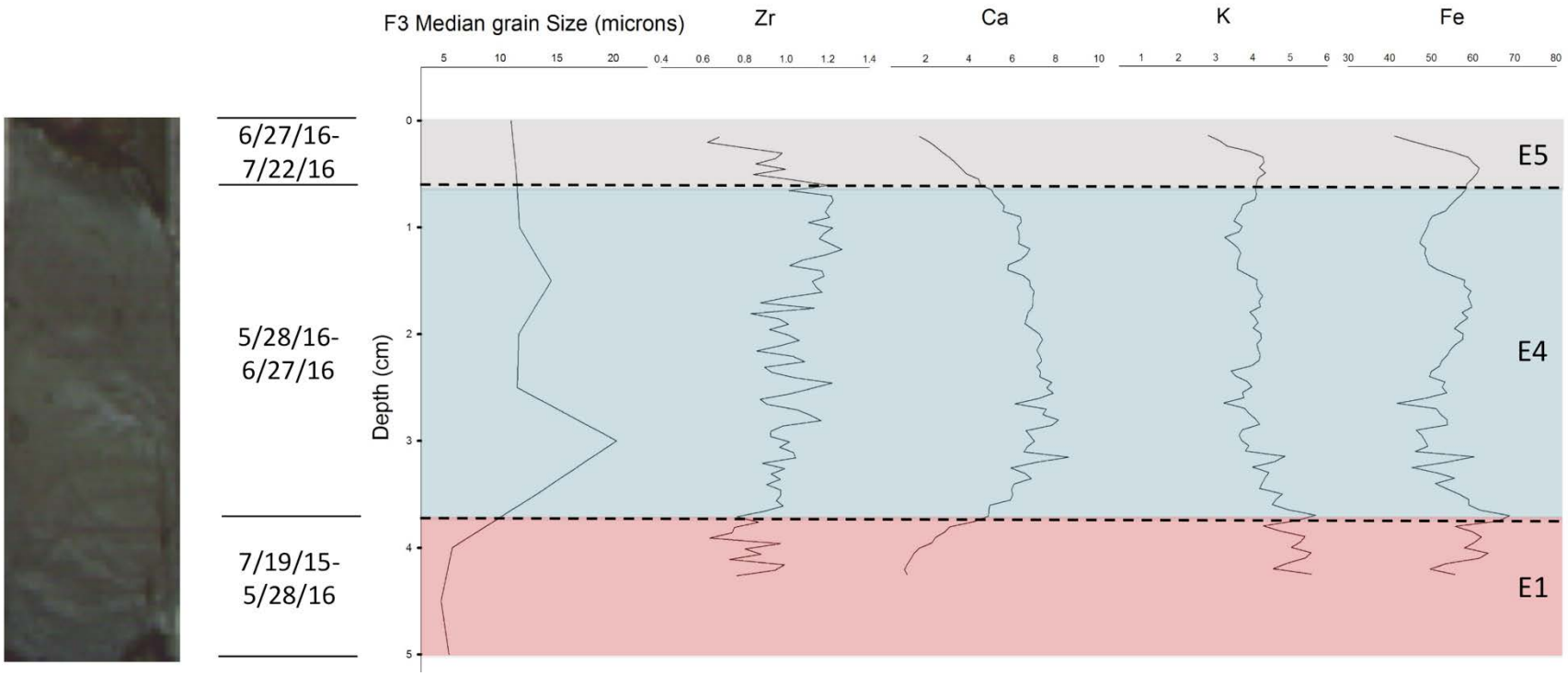


Figure 3.13: ITRAX elemental profiles from trap F3, with E1 and E4-E5 marked. Sediment signatures from E2 and E3 were not present in the core from E. Provided at left are the best known corresponding dates and an image of the core.

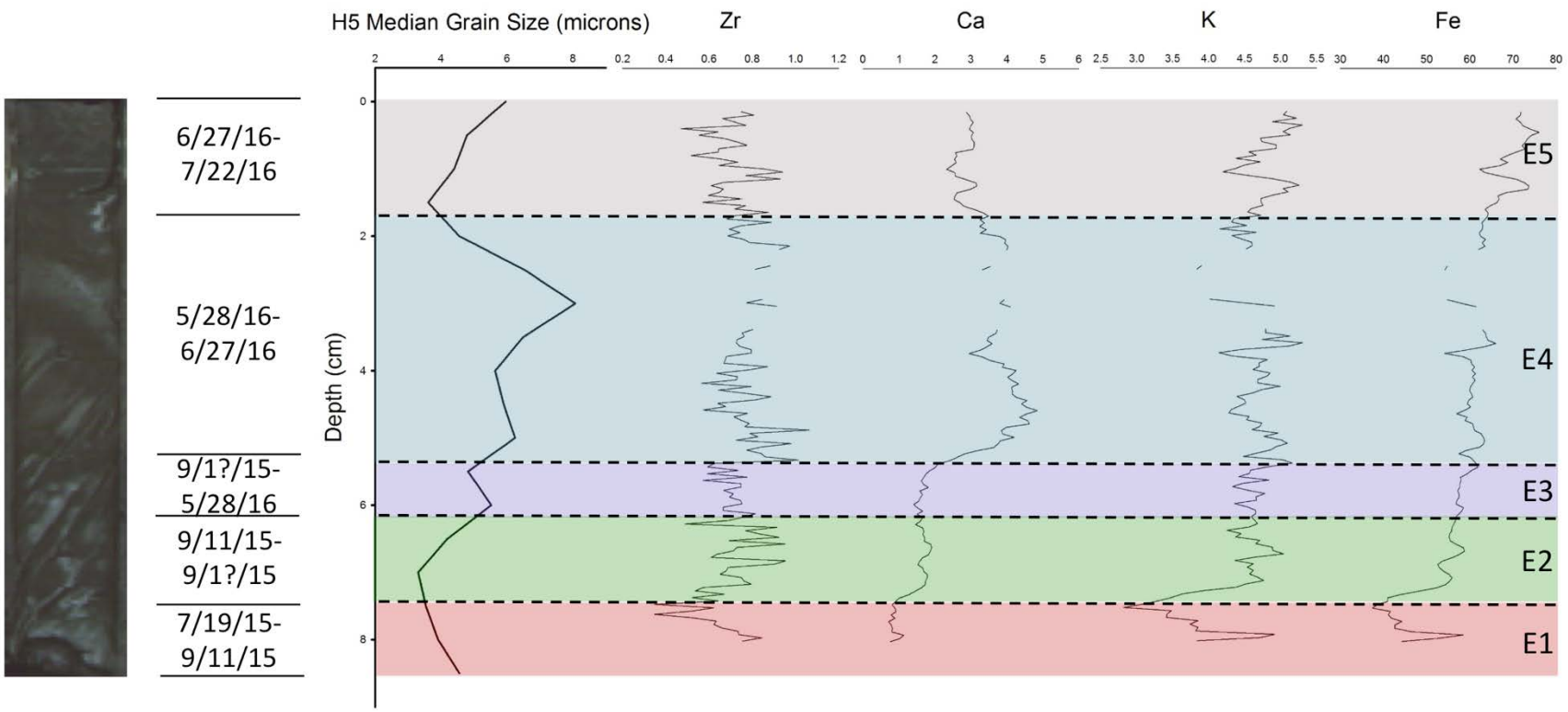


Figure 3.14: ITRAX elemental profiles from trap H5, with E1-E5 marked, the best known corresponding dates, and an image of the core.

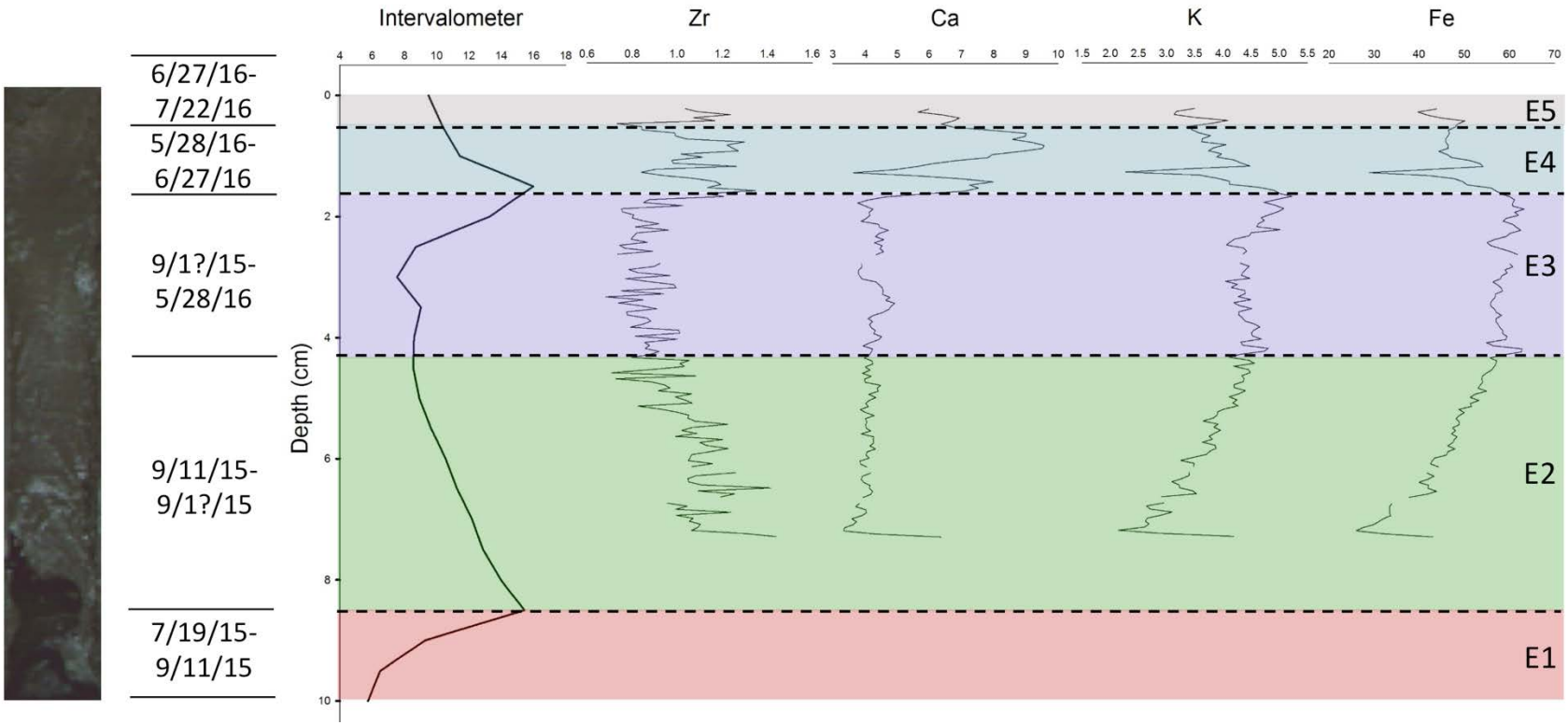


Figure 3.15: ITRAX elemental profiles from the intervalometer core, with E1-E5 marked, the best known corresponding dates, and an image of the core.

# X-Ray Diffraction

Sediment samples from each of the five sedimentation events, E1-E5, were taken from core C4. The samples were characterized by mineralogy using X-ray diffraction, with the relative abundances of different minerals in each sample shown below. While these data indicate with a reasonably high degree of certainty that the listed minerals are present, the relative abundances are presented with a much lower degree of certainty. Quartz is dominant in coarse-grained E2 and E4, and is common in all samples. Muscovite makes up nearly half of fine-grained E3 and E5 and is present as a significant portion of the sediment in the other samples. Kaolinite is present in small amounts in all but E3. Carbonate minerals are present in the middle two samples, with dolomite in E3 and $CaCO_3$ in E4. Clinochore in E1 and E5 and anorthite in E5 make up the remainder of the mineral content of these samples.

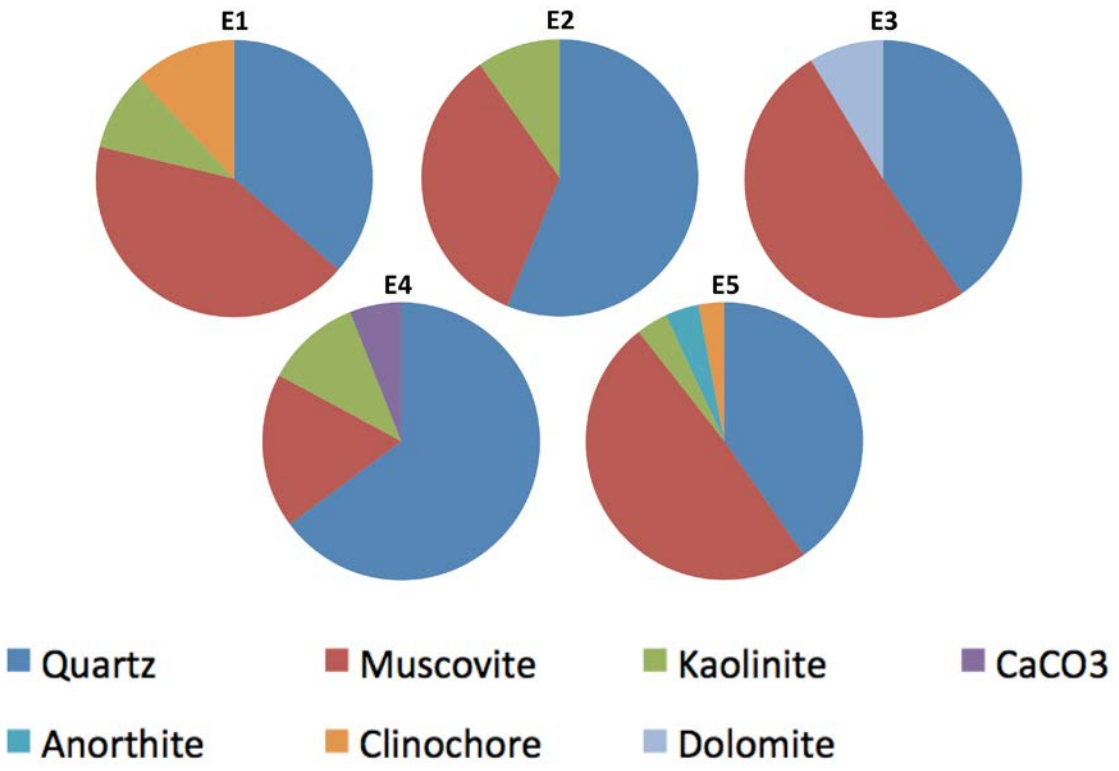


Figure 3.16: Mineral content of E1-E5 in trap C4, from XRF analyses.

# Chapter 4

# Discussion

## Differentiation of Event Signatures in the Sediment Record

With the intervalometer record providing a framework of five distinct sedimentation events, E1-E5, grain size and ITRAX XRF profiles of the sediment traps were used to distinguish which sediment segments were associated with each event. Grain size profiles were used to make preliminary divisions of the sediment cores into distinct segments with boundaries marked by sudden changes in sediment character. High-energy events with coarse-grained signatures were most distinguishable in the grain size data, marked by sharp increases in grain size following periods of much finer-grained sediment deposition. Depositional events with finer-grained signatures such as E3 were at times indistinguishable from other events on the basis of grain size alone. In these cases the elemental composition profiles from the ITRAX analyses were used to determine the boundary between one fine-grained sediment signature and another. The ITRAX data were also helpful in corroborating interpretations based on grain size. Differentiation of sediment signature was performed first in the core from trap C4, as the large amount of sediment collected made it the trap with highest-resolution record. C4 also had sediment signatures from each of the five events, whereas traps D4, E, and F3 were missing the distinct signatures of some events.

# Sedimentation Events

## E1: Late Summer 2015

From the intervalometer's deployment on 7/19/2015 until 9/11/2015, small amounts of sediment were deposited regularly, over short intervals. This period is interpreted collectively as E1, when late-summer pulses of melt water from Linnébreen and precipitation events frequently carried small deposits of sediment into the lake. The low energy of these small pulses of meltwater left only fine-grained deposits. Apart from thicker sediment packages more proximally and thinner sediment packages more distally, there was little spatial variation across the lake in the signatures from E1. E1 sediment was consistently fine-grained, enriched in K and Fe, poor in Zr and Ca, and relatively homogeneous.

## E2: September Rainstorm

Over a 17-hour period from 9/11 to 9/12, the intervalometer recorded roughly 70% of the sediment deposition for the entire sedimentation year. This sedimentation occurred during an intense rainstorm, which provided the energy needed to wash the large amount of coarse-grained sediment found in the signature of E2 into Linnévatnet. The signature matches what could be expected from such a high-energy event: a large fining-upward sequence, with coarse-grained sediments which settled out of the water column immediately and finer grains deposited above them as they settled out more slowly. The coarsest sediment at the bottom of E2's sediment signature, with a median grain size of about 26 microns, would take just over 10 hours to settle 15 m through the water column, whereas the finest-grained sediment (10-15 microns) at the top of E2's sediment signature would take between one and three days to settle through the same 15 m (calculations after Walther, 2015). When a high-energy event such as a major rainstorm washes a large amount of sediment with variable grain size into a calm depositional basin, as in E2, the dependence of settling velocity on grain size yields a distinct fining-upward sediment package as a marker of the event.

While the large rainstorm of 9/11 and 9/12/2015 provides a good explanation for the high sedimentation event, there were other late-season rainstorms of similar intensity, particularly on 8/23/2015 and 9/28/2015, which do not show a large sediment signature like that seen for the 9/11-9/12 rainstorm. While the other two storms matched or exceeded it in intensity during short periods, the 9/11-9/12 rainstorm had far more total rainfall than the other two, with 49.2 mm of rainfall over 48 hours, as compared with only 26.6 mm during the 8/23 storm and 12.2 mm during the 9/28 storm.

As Favaro and Lamoreaux (2014) found in a catchment in the Canadian high Arctic, sedimentation related to late-season rain events is dependent not only on precipitation and sediment availability, but also on antecedent conditions in the catchment. Only when rainfall leads to soil saturation do major sedimentation events occur. If soil saturation is not achieved, rainfall will run off the landscape with little sediment mobilization, and moisture already present in the soil can be just as important to achieving saturation as the amount of moisture introduced as rain in a given event. In

addition to the 49.2 mm of rainfall during the 9/11 rainstorm itself, 15.4 mm of rain fell in the seven days before the storm, with 4 mm of that coming in the 24 hours before the storm. 24.6 mm of rain fell in the week before the 26.6 mm 8/23 rainstorm, but it mostly fell early in that week, with no rainfall during the day before the major storm. Only 4 mm of rain fell in the seven days preceding the 12.2 mm storm of 9/28, with 1 mm of that during the 24 hours before the storm. With totals of 64.6 mm for the storm and preceding week, and 53.2 mm for the storm and the day preceding, the 9/11-9/12 storm would have been better able to achieve soil saturation and mobilize sediment to the extent seen in the sedimentary record than either the 8/23 storm (storm + week before: 51.2 mm, storm + day before: 26.6 mm) or the 9/28 storm (storm + week before: 16.2 mm, storm + day before: 13.2 mm). The 9/11-9/12 rainstorm stands out from other rain events during the late summer and fall for its exceptionally high rainfall totals, which allowed for soil saturation in Linnédalen and yielded the exceptionally high rates of sedimentation seen during the storm.

Unlike E1, the sediment signature for E2 is not uniform across the lake. While E2 shows a strong coarse-grained signature in trap C4 and the intervalometer, and a somewhat weaker coarse signature in trap H5, traps D4, E, and F3 do not show coarse-grained sediment signatures correlating to E2. This is taken as an indication that the sediment transported during E2 traveled across the lake as a plume, not reaching Mooring D or the western basin where Moorings E and F lie. While E2 sedimentation was dominant at Mooring C and prevalent at Mooring H, if the sediment was spatially constrained in a narrow plume, its overall effect on sedimentation across the lake as a whole may not have been as great as the intervalometer record would seem to indicate.

The time lapse “plume cam” on the eastern shore of Linnévatnet, facing the inlet of Linnéelva, is valuable tool for performing visual checks on interpretations about weather and lake conditions. The camera captured views of the 9/11-9/12 rainstorm linked to E2 (Figure 4.1) and the other two late-season storms which did not produce significant sedimentation at the moorings in this study. A distinct plume of sediment can be seen hugging the southeastern shore of the lake at 5:15 am on 9/11/15, the day of deposition for E2, but by 10:15 am, there appears to be a brown plume spreading farther into the east basin, including the area where Mooring C is located. In the two

photographs taken on 9/12, reflections off of the lake surface and cloud cover distort the images so that it is impossible to tell whether or not there is sediment plume activity at the lake surface on 9/12. While it does not provide perfect images of the sediment distribution across the lake at all times during the storm, the plume cam confirms the interpretation that E2 sediment traveled as a plume for at least a part of the time when the intervalometer was recording deposition.

Images taken following both the 8/22 and 9/28 storms also show distinct sediment plumes hugging the southeastern coast of the lake, though in neither case is there an indication of the plume reaching the more central parts of the basin, where the sediment traps are. These smaller storms may have mobilized some sediment which simply never reached the sediment traps, and thus was not shown in the sedimentary record used in this study.

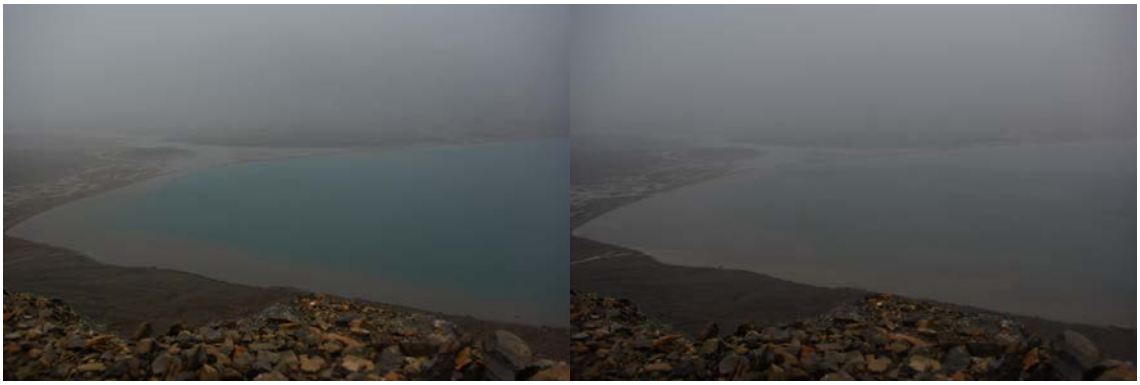

Figure 4.1: Plume cam photographs from E2, the major rainstorm and sedimentation event of 9/11/15. At 5:15 am (left), a narrow plume can be seen hugging the southeast shore of the lake, but sediment has spread across the lake surface by 10:15 am (right).

In the sediment traps where its sediment is present, E2 has a distinct chemical signature. Zr, K, and Fe content all vary with grain size through the fining-upward sequence of E2. Zr content, like grain size, is high at the bottom of the E2 signature and decreases steadily in the upper portions of the sediment package. K and Fe vary inversely with grain size: the bottom of E2's sediment package is poor in both, and both elements increase in prevalence towards the fine-grained top of the sediment package. Ca, unlike the other three elements examined, remains at constant, relatively low levels throughout

the sediment signature of E2, particularly in trap C4, where E2's signature is best defined.

While trap D4 does not have the sharp grain size increase which marks E2 in other traps, an increase in Ca in the long, relatively fine-grained lower half of trap D4 suggests the trap may have received some Ca-enriched sediment from a source other than the coarse-grained plume which reached Moorings C and H. This is especially compelling when considering Mooring D's position very near a fan of carbonate debris on the east coast of the lake, which could have been the source for Ca-enriched sediment. Trap D4 may also have received sediment as the finer grains of the E2 sediment pulse from Linnéelva settled out of the water column slowly. The lower settling velocity of finer grains would provide them more time to dissipate horizontally, away from the original plume extent which did not reach D4 when coarse sediment was settling out.

## E3: Winter Sedimentation Event

There is relatively little sedimentation after the September storm associated with E2 until 1/3/2016, when a small amount of sediment is deposited over the course of about 24 hours in E3. While winter conditions on Svalbard would not usually allow sediment to flow into the lake, the weather record shows a seven-day period from 12/28/2015-1/3/2016 during which air temperatures remained consistently above 0° C, 107.2 mm of rain fell, and ground temperatures at 50 cm depth reached 0° C. This extended period of warm temperatures and increase in ground temperature would likely loosen sediment enough to allow it to be washed into the lake by the rain, and the intervalometer record shows on sediment deposition on 1/3/16. While it is unusual for sediment to be mobilized during January on Svalbard, the weather records show a period of sufficient warmth and rainfall to provide for such an unusual occurrence.

While the thawed ground and flowing water make it possible that new sediment was mobilized in January, another possibility cannot be discounted. The record of sediment deposition from the intervalometer shows single, sudden deposits, rather than a gradual accumulation of sediment. Given the snow and ice restraints on the runoff process, E3 was a relatively low-energy sedimentation event, as indicated by the fine-grained nature of its sediment signature. The median grain size for E3 sediment at

Mooring C is around 10-15 microns, which would take 1-3 days to settle 15 m (calculations after Walther, 2015). Sediment settling for 1-3 days would be most likely to appear in the intervalometer record as a gradual accumulation, not a sudden deposit. Instead of freshly mobilized sediment, the flowing water during this warm period may have dislodged slowly-settling, fine-grained sediment adhering to the funnel walls of the intervalometer during the long period of calm water under the ice before the January rainstorm. A sudden current disrupting sediment and knocking it down into the intervalometer would create the signature of a sudden deposit seen in the intervalometer record. Neither mechanism can be confirmed or discounted as the one responsible or not responsible for deposition during E3 based on the information available, but both should be acknowledged and considered.

Regardless of the mechanism of deposition, the snowy and icy conditions did restrict runoff activity to low energies, and the sediment signature for E3 is accordingly fine-grained. The fine-grained nature of E3 sediment leaves it indistinguishable by grain size alone from the fine-grained upper portion of E2. Instead, the elemental profiles from the ITRAX XRF scans must provide a basis for separating these two segments of fine-grained sediment. The best potential marker of a change in sediment character is a small increase in Fe content near the top of the fine-grained sediment package in trap C4. The increase is also present to varying extents in the other traps along the transect through the eastern basin, but is best defined in C4. Given the lack of strong boundary markers in the sedimentary record, interpretations of the lower boundary location for E3 should be taken to have a high degree of uncertainty. Since there was no signature for E2 in the western basin and the snow and ice at the time of E3 likely would have constrained the flow of any liquid water to Linnéelva, E3 is interpreted to be absent in traps E and F3, though the grain size and ITRAX profiles do not give a definitive answer to the question of whether E3 sediment reached the western basin or not. Like other fine-grained deposits, E3 is rich in K and Fe and poor in Zr. Ca levels in E3 are similar to the moderately low level at which they remained throughout E2's sediment package.

## E4: Nival Flood

A sharp increase and zone of high grain size in the middle or upper portions of all five traps defines E4. On 5/28/2016, sediment began to enter the lake again after a long stagnant period in the winter and early spring months. This is interpreted as the onset of the nival flood, with meltwater from the winter's snowpack flowing again into the lake and carrying sediment with it. Large amounts of meltwater create a high-energy sediment transportation system capable of transporting large sediment grains, which would produce an increase in grain size like that at the lower boundary of E4's sediment signature. Unlike in E2, E4 does not exhibit a fining-upward sequence as its sedimentary signature. Instead, it has a zone of sustained high grain size, with several grain size maxima spaced closely together. The Zr, Ca, Fe, and K content also vary often in this coarse-grained segment, with the higher, 0.5 mm resolution of the ITRAX data showing the variability more clearly than in the 0.5 cm resolution grain size data. These multiple maxima and rapid fluctuations are interpreted as signs of multiple pulses of meltwater carrying numerous small deposits of coarse-grained sediment into Linnévatnet. These may be associated with rainstorms during the spring melt season or simply be the result of particularly warm periods with increased snow melt rates imparting more energy to the fluvial system. The sediment is generally finer more distally, as the coarsest grains settle out of the water column before getting the chance to travel far from the inlet. The signal of multiple pulses during the nival flood is largely overshadowed in the grain size data from Mooring C, as there seems to always be enough energy during the spring melt season to carry coarse sediment the short distance from Linnéelva's mouth to Mooring C. Only during stronger pulses though, is there enough energy to carry coarser grains all the way to the distal Mooring H, so the grain size data in trap H5 record both the strong pulses and the relatively quiet periods in between.

Unlike E2 and E3, the coarse sediment signature for E4 is present across the lake, in all of the sediment traps collected, including E and F3 in the western basin. Whereas E2 sediment apparently entered only from Linnéelva and traveled as a plume, sediment entered the lake from numerous locations during the nival flood and spread out across the lake. This broad spatial distribution was likely aided by the fact that multiple pulses of

meltwater were carrying sediment into the lake at different times, as snow melted all over the valley.

The plume cam photographs (Figure 4.2) for the week leading up to 5/28/16, the day the intervalometer recorded the onset of the nival flood, agree well with the intervalometer record and the weather record, which showed a prolonged period of above-freezing temperatures. On 5/21, the valley was thoroughly covered in snow, with little or no break between the snow on the lakeshore and the snow on the lake ice, and only a few rocks showing through the snow on the valley floor. On 5/28, the day of the first sediment deposition, much of the lakeshore and valley floor is snow-free, with dark rocks showing through the remaining patchy snow. There was also a ring of dark meltwater around the lakeshore on 5/28/16, showing where the edges of the lake ice had partially or completely melted. This included a dark patch at the mouth of Linnéelva, indicating that meltwater from the quickly diminishing snowpack and sediment are indeed able to flow via the river into the lake.

Figure 4.2: Plume cam photographs from 5/21/16 (left), one week before nival flood sedimentation began, and from 5/28/16 (right), the day nival flood sedimentation began.

As stated above, the multiple pulses of the nival flood brought in sediment with varying compositions, but in general, the patterns exhibited previously for Zr, K, and Fe hold true: Zr corresponds to coarse sediment and K and Fe correspond to fine sediment. The Ca signature in E4 stands out, as Ca is much higher in E4 than in any other part of the sediment signature for all parts of the lake. The prevalence of Ca in E4 sediment is discussed further below.

## E5: Return to Summer Melt Conditions

E5 has a small signature much like that of E1, and for good reason: it was produced by the same conditions which brought about E1. After the nival flood's intensity abated, glacial melt and precipitation events remained as the only drivers of sedimentation throughout the summer months. These sporadic, low-energy drivers of sedimentation carried occasional deposits of relatively fine-grained sediment, rich in K and Fe and poor in Zr into Linnévatnet, leaving a sediment signature which would blend well with that of E1, which began around the same time in 2015 that E5 ended in 2016.

# Sediment Provenance

Across traps from the five moorings studied here, several distinct patterns appeared in the elemental composition profiles produced with the ITRAX XRF Core Scanner: Zr correlates positively with grain size, K and Fe correlate negatively with grain size, and high levels of Ca are associated with sediment deposited during the nival flood.

## Zr-Rich Coarse Sediments

Zr covaries well with grain size, as seen in Figure 3.10, depicting grain size and elemental composition profiles for trap C4. Especially telling in the profiles of trap C4 are the increase in Zr content corresponding to the increase in grain size at the base of E2, followed by the steady decline in Zr content along the overlying fining-upward sequence. This finding agrees with those of Croudace, et al. (2006), who list Zr as a marker of turbidite bases and other high-energy deposits, citing its high content in heavy resistate minerals such as quartz. These minerals' high resistance to erosion leaves large, heavy grains which can only be transported in high-energy sedimentation events such as late-season rainstorms or the nival flood. Thus, Zr is left as an elemental marker for coarse-grained sediments carried by high-energy sedimentation events.

The covariance between Zr and grain size is not as well-defined for E4, the nival flood in trap C4, but this likely reflects the previously discussed higher resolution (0.5 mm) for the ITRAX XRF data than for the grain size analyses (0.5 cm) and the multiple,

closely-spaced pulses of spring meltwater. The small, frequent deposits of sediment such pulses bring would leave the pattern of high but variable Zr content while such variations in grain size might be lost in the 0.5 cm resolution of the grain size data. The covariance between Zr and grain size is also weaker in trap H5, the most distal along the transect into the main basin. Like the smaller grain size at H5, this is likely because the largest, most Zr-enriched sediment grains settle out of the water column before reaching Mooring H, leaving the coarsest sediments in H5 with a mineral assemblage poorer in Zr than the coarsest sediments of C4.

XRD analysis of events E1-E5 in trap C4 confirm this hypothesis, as quartz is the dominant mineral in the coarse-grained E2 and E4. Quartz is still common, but in smaller proportions in the finer-grained events. While the quartz could have come from any of the bedrock around Linnédalen, it would be most prevalent in sediments from the quartzite underlying Linnébreen and Linnéelva, in the center of the valley.

## K- and Fe-Rich Fine-Grained Sediments

Contrary to Zr, K and Fe vary inversely with grain size, with high K and Fe content corresponding to low grain size and vice versa. As the ITRAX and grain size profiles (Figures 3.10-3.15) show, fine-grained E1 is marked by exceptionally high K and Fe content, and sharp decreases in both elements correspond to the grain size increase marking the bottom of E2. As grain size slowly decreases in the upper portions of E2 and into E3, K and Fe slowly increase. As with the positive correlation between Zr and grain size, the negative correlation between grain size and K and Fe is weaker in E4. As with Zr though, this can likely be attributed to the multiple pulses of the nival flood and the higher resolution of the XRF profiles showing more detail than the lower resolution of the grain size analyses. Four distinct maxima in Fe and K overlap with the single, wide maximum in grain size that defines E4 in trap C4 (Figure 3.10). These likely represent the previously discussed pulses of stronger and weaker flow and related sediment transportation during the nival flood which were unresolved in the grain size analysis. As with Zr, K and Fe's inverse correlation with grain size is repeated in the other traps, with a weaker correlation in some portions, particularly the nival flood, for the reasons discussed above.

K is interpreted to have come primarily from the fine-grained metamorphic minerals in the phyllites which line the western valley wall. XRD analyses confirm that the fine-grained sediments of E1, E3, and E5 are nearly half muscovite, as would be expected in sediment derived from fine-grained metamorphic rocks. This signature is seen even in the eastern basin, in areas shielded from direct contact with the western valley walls, so at least some of the fine, K-rich sediment is likely being washed downstream from unconsolidated sediment on the valley floor farther south, near the upstream sections of Linnéelva.

Fe is interpreted to have precipitated out of the anoxic bottom waters as FeS, as described by Davison and Heaney (1978). This anoxia occurs when mixing of the lake water stops, as when ice covers the lake in winter, allowing fine-grained sediment to settle out of the water column. The lake water stratifies, and FeS precipitates out of the anoxic bottom waters to join the fine sediments. S data was not collected with the ITRAX scanner, and the XRD data did not yield enough data about Fe-bearing minerals to confirm or cast doubt upon any hypotheses about its origin in the fine sediments. Clinochore was present in small amounts in the fine sediments of E1 and E5, but there was no Fe-bearing mineral identified in other Fe-bearing fine sediments, so the source of the Fe in fine sediments remains open to a variety of hypotheses.

## Ca-Rich Nival Flood Sediment

Ca content is low in the summer months, during the events interpreted as sedimentation from meltwater pulses off of the glacier (E1 and E5). Ca content is higher, and remarkably steady throughout E2 and E3, regardless of grain size. Ca content is especially high in E4, the nival flood, and its signature is distinct enough to serve as a good marker for E4. This trend of Ca as a marker for E4 is repeated across all moorings, and even served as a means of refining the delineation of E4 in trap H5. As shown in Figure 3.14, the grain size profile for trap H5 has a smaller increase in grain size, followed by a large one in the upper portion where E4's signature should appear. While an initial interpretation might find that the larger, higher grain size maximum comprised the signature for E4 in its entirety, the beginning of the broad maximum in Ca, a marker for E4 across the lake, aligns with the first, smaller grain size increase. This indicates that

both grain size peaks are part of the signature for E4, and supports the interpretation above that E4 may have entered the lake in multiple pulses of varying strength, with varying sediment characteristics, and the grain size signature may have been lost to the resolution of the grain size analyses or to poorly-defined boundaries between the sediment associated with the small, repeating pulses of sediment.

Ca can be confidently attributed to the carbonate bedrock assemblage on the eastern valley wall, but with knowledge of Ca-rich sediment in the valley, Ca was expected to be highest during the 9/11 rainstorm, when most of the sediment in the valley was thawed and soil saturation and runoff could mobilize sediment around the entire basin. Instead, the Ca was most prevalent during the nival flood, when large amounts of water were coming down Linnéelva. The Ca is postulated to have come from a fan of unconsolidated sediment extending towards the river from the eastern valley wall. The river's high stage during the nival flood would have mobilized some of this unconsolidated sediment and carried it downstream to the lake. XRD analyses indicate that the Ca in E4 was primarily from $CaCO_3$, but without better data about the surficial geology of the areas upstream in the valley, it remains difficult to pinpoint the exact source of the Ca in E4.

# Conclusions

As recent work (Nowack and Hodson, 2013; Bintanja and Andry, 2017) has shown, "shoulder season" rain events are driving an overall increase in precipitation in the Arctic and on Svalbard especially, becoming more common and more intense as temperatures stay warmer through the fall and into the early winter. The work of Retelle, et al. (2017, Figure 4.3) and Schiefer, et al. (in review, ESPL) shows that this trend can already be seen in Linnévatnet, as four of the last five seasons (2011, 2013, 2014, and 2015) in the sediment trap record have been dominated by fall rainstorms rather than by the spring nival flood. From 2004-2010, nival flood sedimentation dominated the sediment trap record. The trend towards fall rain-driven sedimentation appears likely to have continued in the time since the sediment trap records in this study were collected, as major October and November 2016 rainfall events in Longyearbyen made those months

the warmest and wettest October and November on record for the town, with major debris flows and sediment mobilization associated with both storms. The warm, wet weather was not limited to the fall, as rivers were flowing in Longyearbyen in February 2017 (Retelle, et al., 2017), when they are usually frozen. Based only on these newsworthy weather events, it is reasonable to predict that the 2016-2017 sediment trap record will again be similar to the one analyzed here.

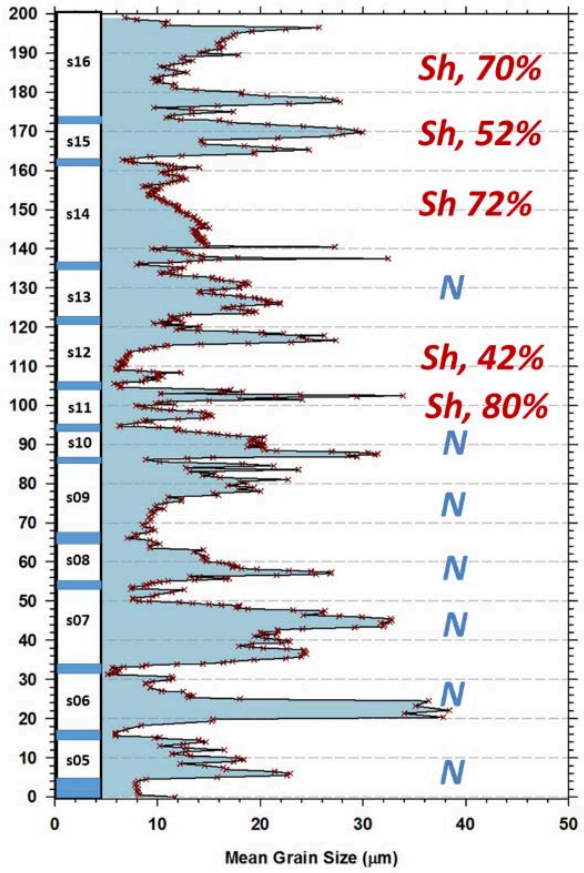


Figure 4.3: The combined sediment trap record from 2004-2016, showing the shift from nival flood-dominated sedimentation to fall rainstorm-dominated sedimentation in recent years, from Retelle, et al. (2017).

If, as it appears, Svalbard and the Arctic are shifting to a climate of fall and winter rainstorms and warm spells, understanding the changes this shifting climate drives in sedimentation patterns will be essential to those studying lake sedimentation in the

Arctic, particularly those continuing work in Linnévatnet itself, whether for paleoclimate reconstruction or understanding of modern climate and sedimentation patterns. The distinctions found between the signatures of different sedimentation regimes in this study can be instructive to those working on lakes like Linnévatnet in the future. The fining-upward sequence of the single, large sediment package from the fall rainstorm stands in contrast with sediment of more variable grain size and composition brought into the lake by may small meltwater pulses during the nival flood. While the fall rainstorm had a dramatic impact where its signature was seen in the sedimentary record, its effects were spatially constrained when it traveled in a plume rather than spreading out across the whole lake, as the signature of the nival flood did. With a high-resolution tool like the ITRAX scanner, The ability to use Zr as a proxy for coarse-grained, quartz-rich sediment and K and Fe as proxies for finer-grained sediment dominated by minerals from the phyllites and other metamorphic rocks on the western valley wall of Linnédalen will be valuable for sediment interpretation in future studies. Ca cannot be confidently predicted to consistently be as prevalent in the nival flood sediments as it was in spring 2016, but ongoing studies would benefit from pinpointing the source of the Ca, perhaps with surficial geologic mapping, and determining whether or not the Ca signature in the nival flood is a recurring trend or a one-time occurrence. It is hoped that the characterization of the sediment trap record in this study aids future research as the climate, hydrology, and sedimentation patterns of Svalbard shift with the warming climate.

# Works Cited

Arnold, M., 2009, Sedimentation in High-Arctic Lake, Linnèvatnet, Svalbard: A Modern Process Study Using Sediment Traps: Bates College Unpublished Thesis.

Asper, V.L., 1987, A review of sediment trap technique: Marine Technology Society Journal, v. 21, no. 2, p. 18-25.

Bintanja, R., and Andry, O., 2017, Towards a rain-dominated Arctic: Nature Climate Change v. 7, p. 263-267.

Bird, B.W., Abbott, M.B., Finney, B.P., and Kutchko, B., 2008, A 2000 year varve-based climate record from the central Brooks Range, Alaska: Journal of Paleolimnology, v. 41, p. 25-41.

Bøyum, A., and Kjensmo, J., Physiography of Lake Linnévatn, Western Spitsbergen, in Proceedings: 20th Congress, Internationale Vereinigung fur Theoretische und Angewandte Limnologie 1978.

Cockburn, J.M.H., and Lamoreaux, S.F., 2008, Inflow and lake controls on short-term mass accumulation and sedimentary particle size in a High Arctic lake: implications for interpreting varved lacustrine sedimentary records: Journal of Paleolimnology, v. 40, p. 923-942.

Cohen, J., Screen, J. A., Furtado, J. C., Barlow, M., Whittleston, D., Coumou, D., Francis, J., Dethloff, K., Entekhabi, D., Overland, J., and Jones, J., 2014, Recent Arctic amplification and extreme mid-latitude weather: Nature Geoscience, v. 7, p. 627-637.

Chutko, K.J., and Lamoreaux, S.F., 2008, Identification of coherent links between interannual sedimentary structures and daily meteorological observations in Arctic proglacial lacustrine varves: potentials and limitations: Canadian Journal of Earth Sciences, v. 45, p. 1-13.

Croudace, I.W., Rindby, A., and Rothwell, R.G., ITRAX: description and evaluation of a new multi-function X-ray core scanner: from Rothwell, R.G., 2006, *New*

*Techniques in Sediment Core Analysis.* Geological Society, London. Special Publications, 267, p. 51-63.

Dallmann, W.K. (Ed.), 2015: Geoscience Atlas of Svalbard. Norsk Polarinstitutt.

Dallman, W.K., Hjelle, A., Andresen, A., Ohta, Y., Salvigsen, O., 1992, Geological Map of Svalbard 1:100 000 B9G Isfjorden: Norsk Polar Institutt, Temakart nr. 16

Davison, W., and Heaney, S.I., 1978, Ferrous iron-sulfide interactions in anoxic hypolimnetic waters: Limnology and Oceanography, v. 23, i. 6, p. 1194-1200.

Favaro, E.A., and Lamoreaux, S.F., 2014, Antecedent controls on rainfall runoff response and sediment transport in a high Arctic catchment: Geografiska Annaler: Series A, Physical Geography, DOI: 10.1111/geoa.12063.

Førland, E., Benestad, R., Hanssen-Bauer, I., Haugen, J.E., Skaugen, T.E., 2011, Temperature and Precipitation Development at Svalbard 1900-2100: Advances in Meteorology, v. 2011, 14 p.

Førland, E., Hanssen-Bauer, I., and Nordli, P., 1997, Climate statistics and longterm series of temperature and precipitation at Svalbard and Jan Mayen: DNMI report, v. 21, no. 97, p. 43.

Frederiksen, L.M., 2017, Changes in lake ice phenology at Linnévatnet, a fresh water lake in the high Arctic of Svalbard: poster, 47th Arctic Workshop, Buffalo, NY.

Hambley, G. W. and Lamoreaux, S. F., 2006, Recent summer climate recorded in complex varved sediments, Nicolay Lake, Cornwall Island, Nunavut, Canada: Journal of Paleolimnology, v. 35, p. 629-640.

Humlum, O., 2002, Modelling late 20th century precipitation in Nordenskiold Land, Svalbard, by geographic means: Norsk Geogra sk Tidsskrift-Norwegian Journal of Geography, v. 56, p. 96-103.

Humlum, O. I., A.; Sollid, J. L., 2003, Permafrost in Svalbard: a review of research

history, climatic background and engineering challenges: Polar Research, v. 22, no. 2, p. 191-215.

Ingolfsson, O., and Landvik, J. Y., 2013, The Svalbard-Barents Sea ice-sheet – Historical, current, and future perspectives: Quaternary Science Reviews, v. 64, p. 33-60.

Isaksen, K., Nordli, Ø., Førland, E. J., Łupikasza, E., Eastwood, S., and Niedzwiedsz, T., 2016, Recent warming on Spitsbergen – Influence of atmospheric circulation and sea ice cover: Journal of Geophysical Research: Atmospheres, v. 121, p. 11,913-11,931.

Kaufman, D. S., Schneider, D. P., McKay, N. P., Ammann, C. M., Bradley, R. S., Briffa, K. R., Miller, G. H., Otto-Bliesner, B. L., Overpeck, J., T., Vinther, B. M., and Arctic Lakes 2k Members, 2009, Recent Warming Reverses Long-Term Arctic Cooling: Science, v. 325, p. 1236-1239.

Lamoreaux, S.F., and Gilbert, R., 2004, A 750-yr record of autumn snowfall and temperature variability and winter storminess recorded in the varied sediments of Bear Lake, Devon Island, Arctic Canada: Quaternary Research, v. 61, p. 134-147.

Mangerud, J., Svendsen, J.I., 1990, Deglaciation chronology inferred from marine sediments in a proglacial lake basin, western Spitsbergen, Svalbard: Boreas, v. 19, p. 249-272.

McCabe, C., 2016, High resolution XRF sediment analysis of late season precipitation events in a High Arctic glaciated watershed: Svalbard, Norway [Bachelor's thesis]: Bates College, 163 p.

Nilsen, F., Skogseth, R., Vaardal-Lunde, J., and Inall, M., 2016, A Simple Circulation Model: Intrusion of Atlantic Water on the West Spitsbergen Shelf: Journal of Physical Oceanography, v. 46, p. 1209-1230.

Nowak, A., and Hodson, A., 2013, Hydrological response of a High-Arctic catchment to changing climate over the past 35 years: a case study of Bayelva watershed,

Svalbard: Polar Research, v. 32, no. 0.

Polyak, L., and M. Jakobsson, 2011, Quaternary sedimentation in the Arctic Ocean: Recent advances and further challenges: Oceanography, v. 24, no. 3, p. 52–64.

Retelle, M., McCabe, C., Roof, S., Walther, T., and Werner, A., 2015, Hydroclimatic controls on laminated sediment formation in Linnévatnet, Svalbard: poster, American Geophysical Union Fall Meeting, San Francisco, CA.

Retelle, M., Potter. N.L., Roof, S., and Werner, A., 2017, Recent hydrological response of a glacierized watershed to high Arctic warming , Linnévatnet, Svalbard: poster, 47th Arctic Workshop, Buffalo, NY

Schiefer, E., Kaufman, D., McKay, N., Retelle, M., Roof, S., and Werner, A., Fluvial sediment yields over hours to millennia in the high Arctic at proglacial lake Linnévatnet, Svalbard: in review, Earth Surface Processes and Landforms (3.5).

Serreze, M., and Barry, R., 2011, Processes and impacts of arctic amplification: A research synthesis: Global Planet. Change, v. 77, p. 85–96.

Serreze, M.C., and Francis, J.A., 2006, The Arctic Amplification Debate: Climatic Change, v. 76, i. 3, p. 241-264.

Snyder, J.A. ,Werner, A., Miller, G. H., 2000, Holocene cirque glacier activity in western Spitsbergen, Svalbard: sediment records from proglacial Linnévatnet: The Holocene, v. 10, no. 5, p. 555-563.

Svendsen, J. I. M., and Mangerud, J., 1997, Holocene glacial and climatic variations on Spitsbergen, Svalbard: The Holocene, v. 7, no. 1, p. 45-57.

Svendsen, J. I. M., J.; Miller, G. H., 1989, Postglacial marine and lacustrine sediments in Lake Linnevatnet, Svalbard: Polar research, v. 5, p. 281-283.

Walther, T., 2015, Analysis of sediment traps in Linnévatnet, Svalbard for reconstruction of annual sediment flux and lacustrine processes [Bachelors thesis:

Bates College].

Woo, M. K., and McCann, B. S., 1994, Climatic variability, climatic change, runoff, and suspended sediment regimes in northern Canada: Physical Geography, v. 15, no. 3, p. 201-226.

Zolitschka, B., Francus, P., Ojala, A. E., and Schimmelmann, A., 2015, Varves in lake sediments–a review: Quaternary Science Reviews, v. 117, p. 1-41.